Linking tephrochronology and soil characteristics in the Sila and Nebrodi mountains, Italy

Gerald Raab[a], Dieter Halpern[a], Fabio Scarciglia[b], Salvatore Raimondi[c], Kevin Norton[d], Thomas Pettke[e], Jörg Hermann[e], Raquel de Castro Portes[a], Asel Maria Aguilar Sanchez[f], Markus Egli[a],*

[a] Department of Geography, University of Zurich, Winterthurerstrasse 190, 8057 Zurich, Switzerland
[b] Department of Biology, Ecology and Earth Sciences (DiBEST), University of Calabria, Via P. Bucci – Cubo 15B, 87036 Arcavacata di Rende, CS, Italy
[c] Dipartimento dei Sistemi Agro-Ambientali, Universitá degli Studi di Palermo, Viale delle Scienze, 90128 Palermo, Italy
[d] School of Earth and Environment, Victoria University of Wellington, PO Box 600, 6140 Wellington, New Zealand
[e] Institute of Geological Sciences, University of Bern, Baltzerstrasse 1 + 3, 3012 Bern, Switzerland
[f] Institute for Building Materials, ETH Zurich, 8093 Zurich, Switzerland

ARTICLE INFO

ABSTRACT

Recent studies have demonstrated that soils formed on pyroclastic ash deposits are much more common in the Mediterranean area than previously assumed. These soils are an important key to understanding past volcanic events and landscape evolution. Chronological information in soils of Quaternary volcanic events, however, remains still poorly understood in southern Italy. Using a multi-method forensic approach, we explore the origin and age of volcanic deposits (soils) in Sicily and Calabria. The geochemical signature of the soil was compared to the chemical fingerprint of the magmas of potential source areas of southern Italian volcanoes. The results indicate that the investigated soils on the Nebrodi (Sicily) and Sila (Calabria) mountains were both impacted by materials having a high-K calc-alkaline series volcanism. The Aeolian Islands (in particular Lipari and Vulcano) are the most likely source of origin, but contributions also from the Etna (particularly the Biancavilla ignimbrites and Plinian eruptions) occurred. Weathering and leaching processes, along with a potential contribution from the underlying non-volcanic bedrock, has altered the main chemical composition of soils, often precluding direct relation to potential source areas. Immobile elements and their ratios (e.g. the Nb/Y vs Zr/Ti plot) or trace elements (Co, Th) and rare earth elements (laser ablation ICP-MS analyses of glass particles, volcanic clasts and pumice-like materials) gave precious hints of the origin of the volcanic deposits. Radiocarbon dating of the H_2O_2 resistant soil organic fraction indicates a minimum age of 8–10 ka of the soils. The weathering index WIP (weathering index according to Parker) and the chemical composition of volcanic glasses and clasts were tested as proxies for the age of the volcanic deposits and time for soil formation. The soils and landscape are characterised by multiple volcanic depositional phases for the last about 50 ka in the Sila mountains and about 70 ka or more in the Nebrodi mountains. Chemical-mineralogical analyses enabled the detection of deposition phases during the Pleistocene and also Holocene. The multi-method approach enabled the identification of potential source areas, provided a tentative age estimate of the start (and in part duration) of ash deposits and therefore improved our understanding of volcanic landscape evolution.

1. Introduction

Volcanic eruptions are spectacular natural events (Giaccio et al., 2008) that have captured man's curiosity since prehistoric times. On the one hand, they can be of great benefit to man (e.g. increased soil fertility), but on the other hand they can also cause great harm (Fisher and Schmincke, 1984; Sulpizio et al., 2014; Sandri et al., 2016). In a large part of the world, today's landscape has been predominately formed since the late Quaternary period. In those last two and half million years, the Mediterranean region was marked by numerous spectacular natural and highly explosive volcanic events (Paterne et al., 2008; Scarciglia et al., 2008; Bourne et al., 2015). These events have clearly left their marks on the landscapes. Fine volcanic material generally affects large areas around volcanic centers (Giaccio et al., 2008).
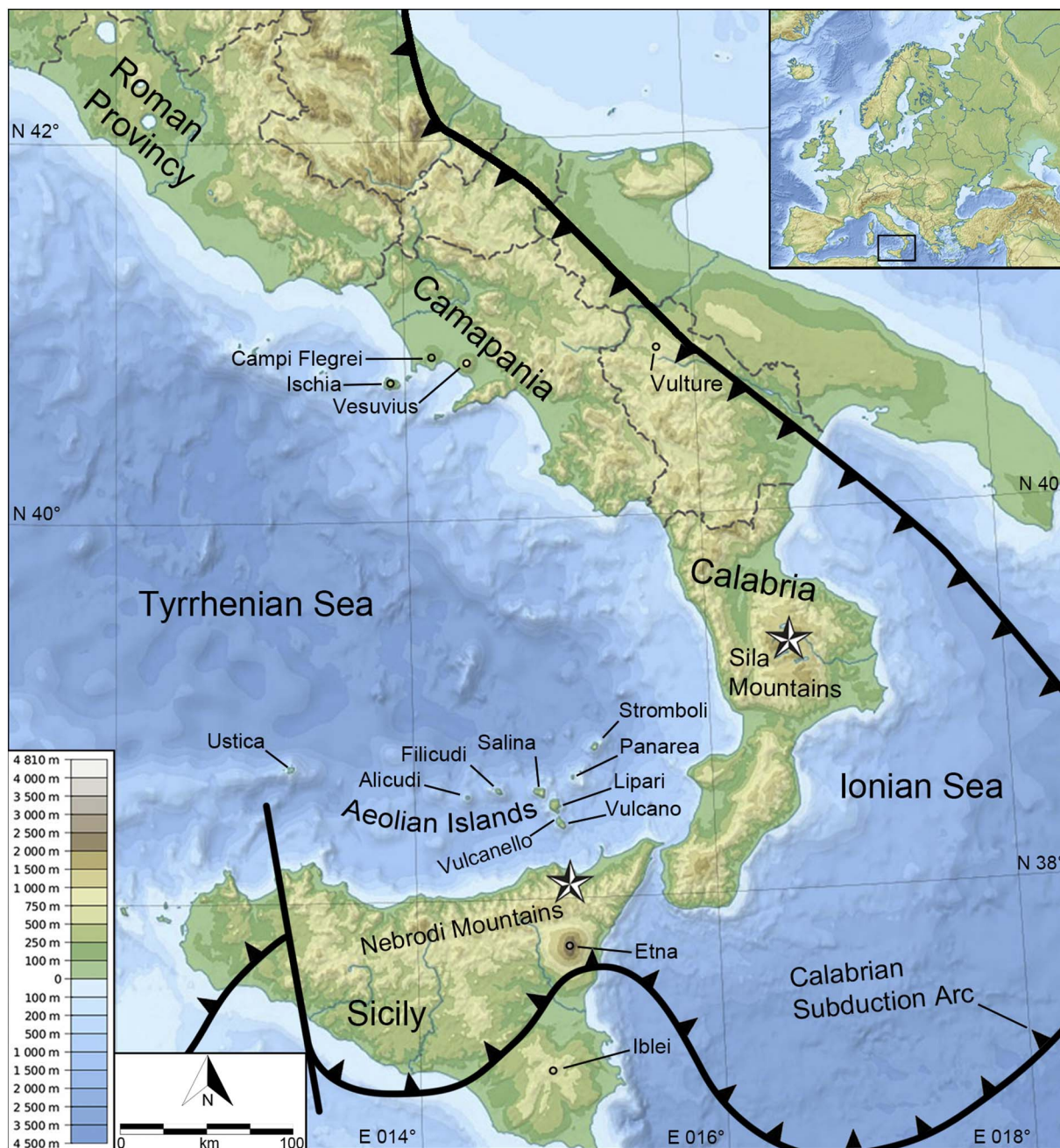
Fig. 1. Location of the study areas. The two stars mark the investigation sites in the Nebrodi and Sila mountains.

Chemical evaluation of this fine grained material is a powerful tool for Quaternary studies, providing not only a target for dating, but also a means to correlate specific deposits to a specific source, sometimes located at a great distance (Giaccio et al., 2008). According to Zimmerer et al. (2016), information about timescales of magmatism and ages of eruptions is crucial to understanding the history as well as the hazards of active and dormant volcanic areas. These authors also claim that knowledge of eruption ages can be further used to calculate hazard parameters such as recurrence intervals and repose periods, as well as to identify vent migration patterns that are crucial to eruption forecasting. In spite of their social and geological importance, chronologies for Quaternary volcanic events remain poorly understood (Zimmerer et al., 2016). To date, several numerical methods have been used for dating volcanic sediments, such as radiocarbon (^{14}C), potassium-argon decay (^{40}K/^{39}Ar), fission-track geochronology, uranium-lead decay (^{235}U/^{207}Pb) or cosmogenic nuclides (^{10}Be).

However, the necessary conditions for successful application of these numerical methods are often not fulfilled and hence relative dating techniques remain an essential tool (Favilli et al., 2009a, 2009b). A multi-method approach, i.e. a combination of numerical analyses and relative dating methods, can possibly yield more accurate results (Giaccio et al., 2008). The Italian Mediterranean Basin is a complex and volcanically active zone in Europe (Pichler, 1984) with abundant ash fall. Despite their wide spread occurrence (about 7% of the soil area has volcanic deposits as parent material; Costantini and Dazzi, 2013), the source of volcanic sediments is still unknown in many areas. Throughout Sicily and mid- to southern-Italy, the large physical presence of volcanic materials is a constant reminder of the intense volcanic activity of the area. The origin of much of this volcanic material is unknown due to the abundance and activity of different volcanoes in close proximity (Giaccio et al., 2008). Here we attempted to trace the origin of volcanic sediments in southern Italy (Sicily/Calabria) and to

Table 1
General characteristics of the study sites Nebrodi (Sicily) and Sila (Calabria) in southern Italy.

Site	Coordinates WGS 84 (N/E)	Elevation m a.s.l.	Geologic substrates along the profile	Vegetation	Slope	Exposure °N	Soil type WRB (IUSS Working Group, 2015)	Land use
Nebrodi mountains – Sicily								
Nebrodi I	37°59′15.5″/14°58′41″	1269	Volcanic deposits, Quartz-arenite	Fen, grass, maquis	0°	0	Vitric Cambisol	Regional park (pasture)
Nebrodi II	37°59′01.6″/14°57′52″	1279	Volcanic deposits (ash, lapilli), marl, Quartz-arenite	Fen, grass, maquis	11°	345	Vitric Cambisol	Regional park (pasture)
Nebrodi III	37°59′05.9″/14°59′17″	1243	Quartz-arenite	Fen, grass, maquis	8°	90	Vitric Andosol	Regional park (pasture)
Nebrodi IV	37°59′02.1″/14°57′51″	1264	Volcanic deposits (ash, lapilli), marl, Quartz-arenite	Fen, grass, maquis	4°	0	Vitric Cambisol	Regional park (pasture)
Sila mountains – Calabria								
Sila I	39°16′50″/16°32′19″	1572	Volcanic deposits, granite	Shrubs, grass	2°	195	Vitric Cambisol	National park (pasture)
Sila II	39°16′50″/16°32′19″	1572	Volcanic deposits, granite	Shrubs, grass	2°	195	Vitric Cambisol	National park (pasture)

derive an approximate age of the timing of their deposition. To this end, we tested the following hypotheses: 1) the chemical signatures of the volcanoes where these sediments originate from can still be found in the soil, 2) radiocarbon dating and weathering indices of the soils can help to constrain the numerical or at least relative age of the deposits of interest.

2. Materials and methods

2.1. Study area

Two investigation sites in southern Italy were chosen for this study (Fig. 1). One site is on the east end of the Nebrodi mountains, Sicily. The second study region is in the centre of the Sila mountain plateau, Calabria. The two sites differ in some aspects. Sila has a granite parent material of the Calabride complex (Cirrincione et al., 2015). In contrast, the bedrock of the Nebrodi mountains derives from the allochthonous flysch basin sequences of the Numidian flysch formation, which also contains quartzarenite sandstones (Thomas, 2011) besides limestone and clays. The Sila (with a max. altitude of slightly above 1900 m a.s.l.) and Nebrodi mountains (highest peaks slightly above 1800 m a.s.l.) have a comparable elevation and climate (Table 1). Both locations are characterised by a Mediterranean warm climate at the lower altitudes and temperate to cool climate at the highest altitudes. Hill tops (at about 1300 m a.s.l.) and hill slopes of the Sila mountains have an annual average temperature of 9–12 °C with an annual precipitation of 1000–1800 mm (Le Pera and Sorriso-Valvo, 2000), and temperatures at high and medium mountain altitudes in Nebrodi ranging between 9 and 13 °C in average, with precipitation rising to over 1000 mm/year (Tuttolomondo et al., 2014; Floresta meteorological station 1250 m a.s.l.: MAAT 9.3°). Looking at plant diversity, Nebrodi is mostly covered by grass, maquis and fen in contrast to Sila where shrubs and grass make up the cover, along with patches of pine- or beech-forest (Table 1).

2.2. Sampling strategy

In total, four profiles (all at a similar altitude of about 1300 m a.s.l.) on the Nebrodi mountains and two profiles on the Sila mountains (at approx. 1500 m a.s.l.; Table 1) were investigated in detail. The soil profiles on the Nebrodi mountains were selected by using ferns as bio-indicators as they are primarily found on acidic substrates which are a common feature of volcanic soils (Siddig et al., 2015). In the Sila mountains, the sites were selected based on already-existing investigations (Scarciglia et al., 2008; Pelle et al., 2013; Vingiani et al., 2014). All soil profiles (Fig. 2) can be considered as representative of

the main soil types. About 1–2 kg per soil horizon (continuous sampling over the horizon) were taken using open pits. In addition, soil cylinders were used to determine bulk density of the soil material. The ash layers in the areas of Nebrodi II and IV and in the area Nebrodi III (Fig. 3a) were mapped and their thickness registered using a Pürckhauer soil corer. The mapped areas were 77,000 m^2 and 26,000 m^2 respectively, and the variability of the ash layer (or Andosol-like epipedon) thickness on the Nebrodi mountains was assessed.

2.3. Physical and chemical analyses

All bulk samples were sieved to < 2 mm (fine earth) after oven drying (70 °C) for 48 h. The soil skeleton represents the weight ratio of the fraction ≥ 2 mm of the total bulk sample. After a pre-treatment of the fine earth with H_2O_2 (3%), particle-size distribution of the fine-earth was measured using a combined method consisting of wet-sieving the coarser particles (2000–32 μm) and determining the finer particles (< 32 μm) by means of an X-ray sedimentometer (SediGraph 5100). The SediGraph was used without autosampler to prevent, as far as possible, a disturbance of the stirring process caused by ferromagnetic material that may be potentially present. Coarse, rounded volcanic material (lapilli), retrieved from the Nebrodi soils, was removed and separately milled for further analyses. Soil pH (in 0.01 M $CaCl_2$) was determined on air-dried fine-earth samples using a soil:solution ratio of 1:2.5. Fe, Al and Mn concentrations were determined (in duplicate) after treatment with NH_4-oxalate (buffered at pH 3; McKeague et al., 1971). The extracts were centrifuged for 8 min at 4000 rpm and filtered (mesh size 0.45 μm, S & S, filter type 030/20). Element concentrations were measured using atomic absorption spectroscopy (AAnalyst 700, Perkin Elmer). Element concentrations were furthermore controlled using standard addition (recovery ≥ 95%). The oxalate (Al_o, Mg_o, Fe_o) treatment extracts both the weakly- and poorly crystalline phases and some of the organic phases, but normally does not dissolve the strong humus-metal complexes (Mizota and van Reeuwijk, 1989). Loss on ignition (LOI) was performed by igniting 2 g of oven-dried fine earth at 1000 °C for 2 h. Measurement of the total element content of fine earth and lapilli and arenite (after crushing) was done by means of X-ray fluorescence (XRF) (Beckhoff et al., 2006). Approximately 5 g of soil material was milled to < 50 μm and analysed as loose powder in sample cups using an energy dispersive X-ray fluorescence spectrometer (SPECTRO X-LAB 2000, SPECTRO Analytical Instruments, Germany). For comparison additional data of analysed glass particles of the Sila soil were provided by Scarciglia et al. (2008). Scanning electron microscopy analyses, coupled with energy dispersive spectroscopy (SEM–EDS), were performed on Au-coated thin sections to assess and characterise volcanic components (Scarciglia et al., 2008). Total
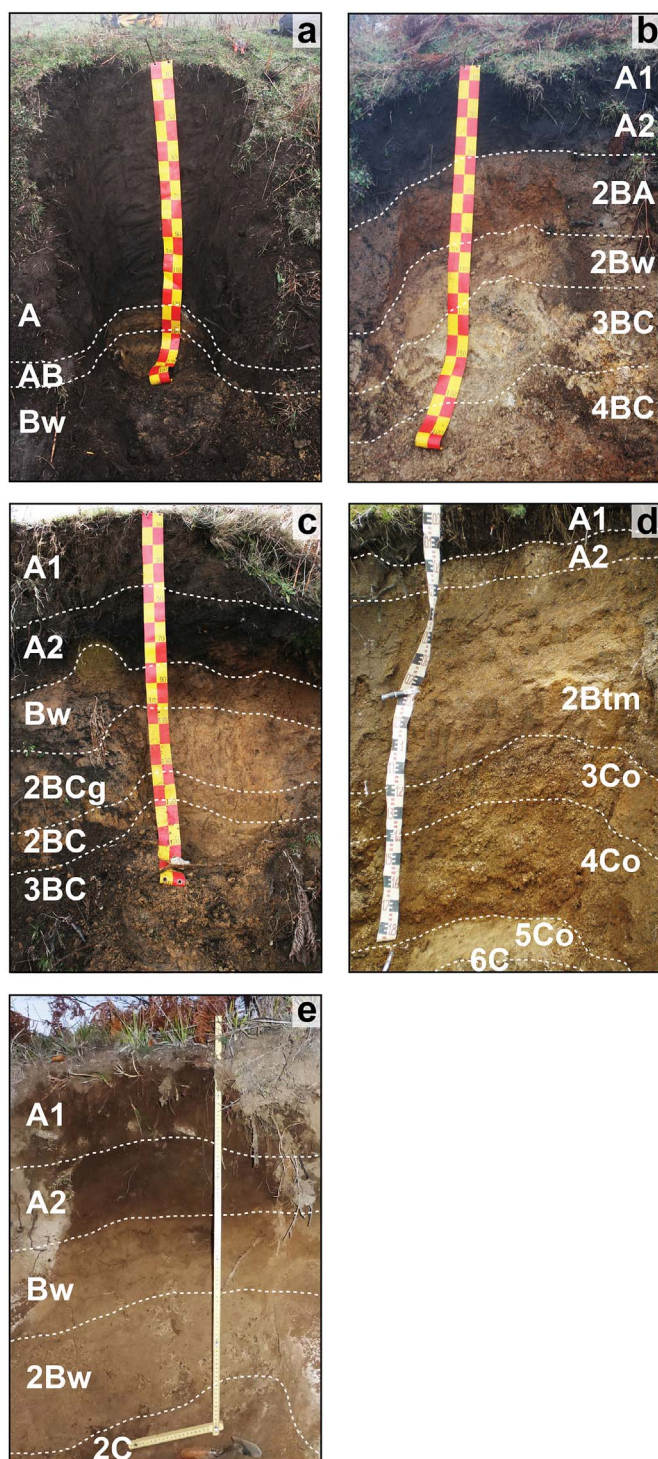
Fig. 2. Soil profiles (with soil horizon designation) at the investigated sites, a = Nebrodi I, b = Nebrodi II, c = Nebrodi III, d = Nebrodi IV and e = Sila II.

organic carbon (C) and nitrogen (N) values were obtained using a Leco® C-H-N elemental analyser (CHNS-932, USA). For this task, oven-dried finely milled soil material was used.

2.4. Soil mineralogy

For a general qualitative overview of soil minerals present, XRD (Bruker AXS D8 Advance, CuKα) and DRIFT (Diffuse Reflection Infrared Fourier Transform; Bruker, Tensor 27) measurements of the fine silt and clay fraction (< 32 μm) were performed. The DRIFT analyses were run

from 250 to 4000 cm^{-1}. About 30 mg of finely-ground soil material and 270 mg of KBr were homogenised in a mill using a fine ball-mill (Zr) for 30 s and at 10 rpm. Prior to measurement, the samples were dried in an oven at 70 °C for 2 h. The individual spectra were interpreted using OPUS 6 software. For X-ray analyses, randomly oriented samples were scanned from 2 to 80°2θ with steps of 0.02°2θ at 10 s intervals using a Bruker AXS D8 Advance (CuKα). The measured spectra were evaluated using DIFFRACplus EVA.

2.5. ESEM-EDS and LA-ICP-MS measurements

Selected samples were polished (up to 1 μm) with a diamond spray and then carbon coated. The SEM analyses were performed using a SEM FEI QUANTA 200 3D under high vacuum and SSD (solid state detector) operating at an accelerating voltage of 20 kV. The energy dispersive X-ray spectroscopy (EDX) was equipped with an Si(Li)EDX Detector that enabled point measurements on volcanic glass particles.

The chemical composition (major and trace elements) of glass particles, pumice and volcanic clasts of selected samples was determined by using a laser ablation ICP-MS (LA-ICP-MS). The system at the University of Bern consists of a Geolas Pro 193 nm ArF Excimer laser (Lambda Physik, Germany) coupled with an ELAN DRCe quadrupole mass spectrometer (QMS; Perkin Elmer, USA). Details on the setup and optimisation strategies can be found in Pettke et al. (2012). Daily optimisation of the analytical conditions were done to satisfy a ThO production rate of below 0.2% (i.e., Th/ThO intensity ratio < 0.002) and to achieve robust plasma conditions monitored by a Th/U sensitivity ratio of 1 as determined on the SRM612 glass standard. Analyses were done using 10 Hz laser repetition rate and 32–90 μm beam sizes, the maximum possible chosen to minimise limits of detection. External standardisation was done employing GSD-1G from USGS, SRM612 from NIST was measured for quality control (employing reference concentrations reported for both in Peters and Pettke, 2017) and bracketing standardisation provided a linear drift correction. Internal standardisation employed the sum of total major element oxides = 97 wt%. Data reduction was done off-line with the SILLS program (Guillong et al., 2008), with rigorous limits of detection calculated for each element in every analysis following the formulation detailed in Pettke et al. (2012).

2.6. Radiocarbon dating

Partial oxidative degradation of organic materials (OM) leaves behind intrinsically resistant as well as mineral-protected OM. This fraction can be extracted using a H_2O_2 leaching protocol (Favilli et al., 2008). This method is based on the oxidation of OM by 10% H_2O_2 (Plante et al., 2004, modified; Eusterhues et al., 2005). 2 g of air-dried, untreated soil (< 2 mm) were wetted for 10 min with distilled water in a 300-ml beaker. Afterwards, 180 ml of 10% H_2O_2 were added. The procedure was run at a temperature of 50 °C in a closed system for 168 h (7 days). Furthermore, additional charcoal samples were taken from two already studied soil profiles (CL4 and 5; cf. Moser et al., 2017). The charcoal samples were treated using the ABOx procedure (Brock et al., 2010; Wood et al., 2012). The ABOx procedure includes a treatment at room temperature in 6 M HCl for 1 h, followed by 2 M NaOH for 30 min, during which time the solution is replaced until it remains colourless. The charcoal is subsequently oxidised in H_2SO_4/ $K_2Cr_2O_7$ (2 M/0.1 M) at 60 °C in a sealed tube for 20 h. The charcoal was washed three times with ultrapure water between each treatment.

The samples (cleaned charcoal and soil sample fractions) were heated under vacuum in quartz tubes with CuO (oxygen source) to remove any absorbed CO_2 in the CuO. The tubes were then evacuated again, sealed and heated in the oven at 900 °C to obtain CO_2. The CO_2 of the combusted sample was mixed with H_2 (1:2.5) and catalytically reduced over iron powder at 535 °C to elemental carbon (graphite). After reduction, the mixture was pressed into a target and carbon ratios were
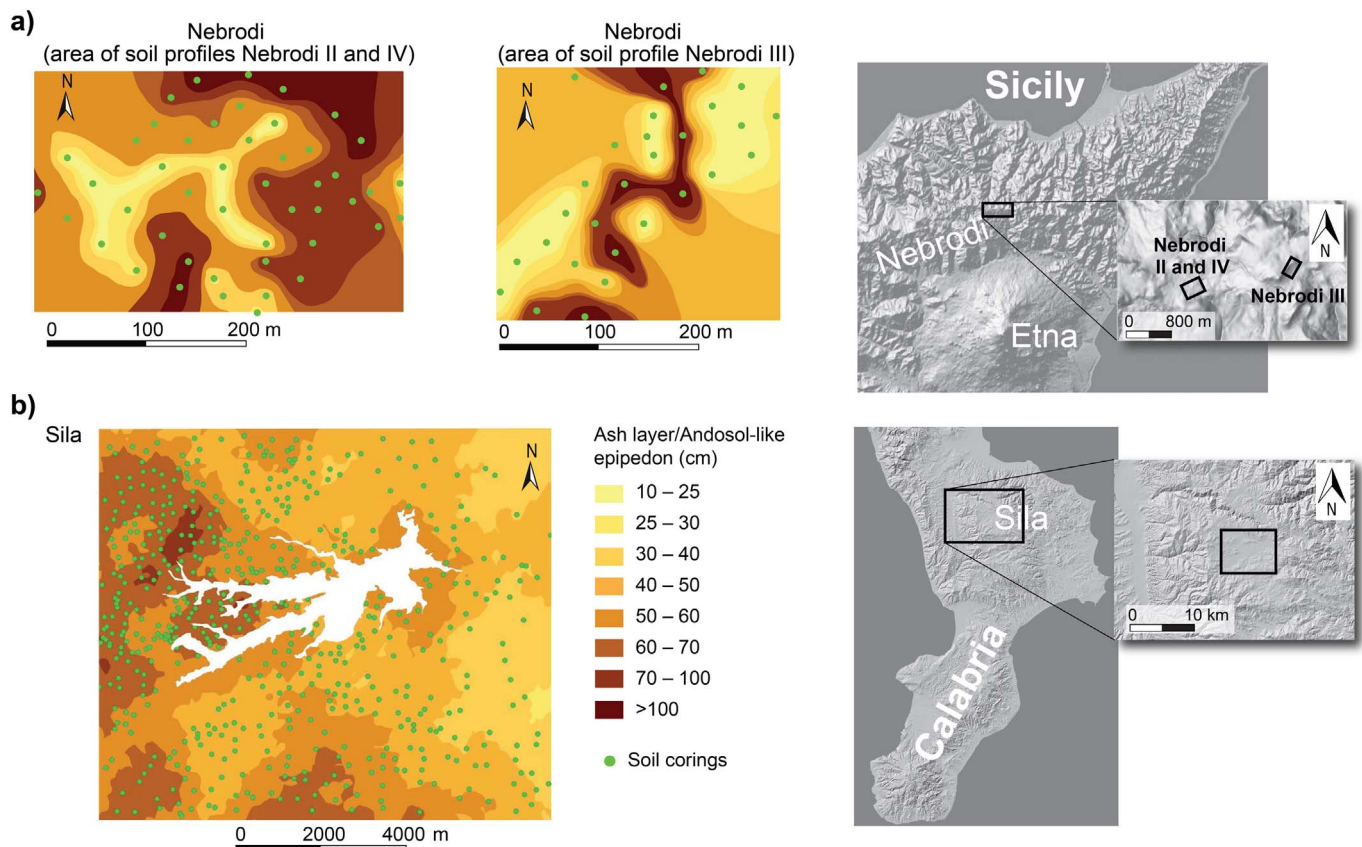
Fig. 3. Maps of ash layer thickness/Andosol-like epipedon based on soil coring investigations a) at the sites Nebrodi II, III and IV and b) around the Cecita Lake (Sila) after Scarciglia et al. (2008). The maps are created based on the DEM 20 SINAnet (Calabria; project SIGIEC, Sistemi Territoriali S.r.l., 2012) and SITR (Sistema Informativo Territoriale Regionale, Regione siciliana).

measured by Accelerator Mass Spectrometry (AMS) using 0.2 MV radiocarbon dating facility (MICADAS) of the Ion Beam Physics at the Swiss Federal Institute of Technology Zurich (ETHZ). The calendar ages were obtained using the OxCal 4.2 calibration program (Bronk Ramsey, 2001, 2009) based on the IntCal 13 calibration curve (Reimer et al., 2013). Calibrated ages are given in the 1σ and 2σ range (minimum and maximum value for each).

2.7. Chemical weathering indices and semi-quantitative and relative dating

To characterise mineral alteration and the weathering degree of soil material several indices have been utilized. According to Parker (1970), weathering and leaching generate a loss of mobile elements over time, and therefore an enrichment of non-mobile elements. Consequently, similar soils within the same geographic position should have a similar index value in the same time span. The older a soil surface the more easily weatherable elements are leached and relatively immobile elements enriched. As such, the bulk chemistry of a given soil should be a function of its age. A large number of such proxies have been proposed and over the years, often with variable relevance for the investigated system. In this study the utility of a number of these geochemical proxies were tested for deriving an age estimation of volcanic-influenced soils. The index B of Kronberg and Nesbitt (1981) and the chemical index of alteration (CIA) of Nesbitt and Young (1982) are based on the same considerations and provide a quantitative measure of feldspar weathering (Buggle et al., 2011). Index B is defined by the molar ratio of:

$$B = \frac{CaO + K_2O + Na_2O}{Al_2O_3 + CaO + K_2O + Na_2O} \tag{1}$$

The CIA is defined as:

$$CIA = 100\left[\frac{Al_2O_3}{Al_2O_3 + CaO + Na_2O + K_2O}\right] \tag{2}$$

The index B and CIA refer to silicate weathering. The investigated soils have all a pH around 5 (Table 2). Consequently, the total CaO content refers to silicate CaO because no carbonates are present. As stated by Dahms et al. (2012) and Egli et al. (2008), the molar ratio of $(K + Ca)/Ti$ can be used to determine the time of surface exposure and can also be deployed as a weathering index, based on the fact that K and Ca are mobile elements, while Ti is considered to be an immobile element because of its higher ionic potential (Egli and Fitze, 2000; Stiles et al., 2003; Buggle et al., 2011). Harnois (1988) presented a CIA without considering potassium because K may either be enriched or depleted in soil. He therefore suggested a chemical index of weathering (CIW):

$$CIW = 100\left[\frac{Al_2O_3}{Al_2O_3 + CaO + Na_2O}\right] \tag{3}$$

In addition the plagioclase index of alteration (PIA) of Fedo et al. (1995), which is an Al-content corrected version of the CIW, was tested together with the WIP (Parker, 1970).

The PIA is given by:

$$PIA = 100\left[\frac{Al_2O_3 - K_2O}{Al_2O_3 + CaO + Na_2O - K_2O}\right] \tag{4}$$

the WIP, calculated by using the weight percent, by (Price and Velbel, 2003):

$$WIP = 100\left[\frac{2Na_2O}{0.35} + \frac{MgO}{0.9} + \frac{2K_2O}{0.25} + \frac{CaO}{0.7}\right] \tag{5}$$

Finally the chemical proxy of alteration (CPA) of Buggle et al.

Table 2
Typical chemical characteristics of the soils.

Site	Horizon	pH (CaCl₂)	C (g/kg)	N (g/kg)	C/N	Al$_o$[a] (g/kg)	Mn$_o$[a] (mg/kg)	Fe$_o$[a] (g/kg)	Al$_o$ + 1/2Fe$_o$ (g/kg)
Nebrodi I	A1	4.92	110.0	9.62	11.4	7.86	497	5.95	10.84
	A2	4.69	94.3	8.23	11.5	10.68	524	6.03	13.70
	A3	4.72	72.4	6.40	11.3	11.74	581	6.82	15.15
	A4	4.85	72.5	6.26	11.6	9.66	459	6.05	12.69
	AB	4.82	9.5	0.51	18.5	1.03	202	2.15	2.11
	Bw	4.68	3.9	0.16	24.4	0.36	169	0.73	0.73
Nebrodi II	A1	5.76	48.1	3.83	12.6	4.94	750	6.95	8.42
	A2	5.62	66.0	4.51	14.6	14.57	856	7.410	18.28
	2BA	4.95	32.4	1.94	16.7	38.41	604	23.26	50.04
	2Bw	4.92	44.0	3.16	13.9	63.32	716	23.21	74.93
	3BC	4.42	3.1	–	–	1.22	1005	3.71	3.08
	4BC	4.02	3.0	0.04	–	0.86	3	2.83	2.28
Nebrodi III	A1	4.99	19.1	1.32	14.4	1.45	180	1.91	2.41
	A2	4.75	40.2	2.40	16.8	11.28	356	7.50	15.03
	Bw	4.73	9.5	0.34	28.3	10.86	214	6.67	14.20
	2BCg	4.28	2.4	–	–	0.93	233	2.19	2.03
	2BC	4.07	2.7	0.11	24.3	0.86	197	1.68	1.70
	3BC	3.92	2.6	0.00	–	1.22	254	2.04	2.24
Nebrodi IV	A1	5.00	32.1	2.84	11.3	10.49	453	5.31	13.15
	A2	5.00	11.9	1.21	9.9	22.96	425	7.15	26.54
	2Btm	4.75	10.8	1.00	10.7	1.35	361	13.01	7.86
	3Co	5.10	5.7	0.69	8.2	10.64	537	11.09	16.19
	4Co	5.30	4.3	0.57	7.6	6.81	1446	16.45	15.04
	5Co	5.75	1.5	0.57	2.7	0.30	1013	2.76	1.68
	6C	4.50	3.4	0.53	6.4	–	23	2.13	–
Sila I	A1	4.80	58.6	4.45	13.2	5.73	326	4.21	7.84
	A2	5.00	39.1	2.98	13.1	6.77	306	4.00	8.77
	Bw	5.00	13.2	1.18	11.2	8.83	59	1.23	9.45
	2Bw	5.10	7.9	0.75	10.5	9.95	13	0.42	10.16
	2C	4.90	4.2	0.47	8.9	9.21	32	0.23	9.33
Sila II	A1	5.13	52.6	3.64	14.4	4.18	340	3.96	6.16
	A2	5.01	35.3	2.39	14.8	4.20	385	11.72	10.06
	Bw	5.08	19.4	1.21	16.1	6.65	50	2.14	7.72
	2Bw	5.23	5.2	0.05	–	1.23	25	0.42	1.44
	2C	5.24	5.4	–	–	5.48	11	0.08	5.52

[a] Oxalate-extractable fraction.

(2011) was also tested.

$$CPA = 100 \left[\frac{Al_2O_3}{Al_2O_3 + Na_2O} \right] \tag{6}$$

Semi-quantitative dating was achieved by using weathering data (total elemental contents and calculation of weathering indices) given in Mirabella et al. (2005) and relating this dataset to numeric surface ages (also provided in Mirabella et al., 2005). Using regression curves (weathering indices vs surface age) an age estimation could be performed for sites (or soil horizons) having a given geochemical composition of the same source but unknown ages.

3. Results

3.1. General soil characteristics

The investigated soils had an upper mineral A horizon and showed typical features of volcanic soils having vitric properties (Table 1). The displayed colours in the A horizons – according to the Munsell soil colour charts – ranged from black to dark brown in wet conditions, when dry, the soils displayed lighter colours (Table 3). Nebrodi I has in the topsoil a relatively high silt content (loam) and in the subsoil the material is sandier (sandy loam). The profile is mainly made of volcanic ash and has one massive umbric (10YR1.7/1) A horizon that extends from the top to 130 cm depth, followed by two more, but comparatively shallower, horizons. Furthermore, the soil is slightly acidic. Soil profile Nebrodi II is characterised by loam, sandy clay loam or sandy loam textural classes (Soil Survey Division Staff, 2010). The site Nebrodi II has a sandy loam or loam texture all over the profile. Also Nebrodi II

has two umbric (7.5YR3/1 and 7.5YR7/1) A-horizons, which predominantly consist of ash material and extend from the surface to a depth of 50 cm. Similarly to Nebrodi I and II, Nebrodi III has two dark (umbric) (10YR3/2 and 10YR1.7/1) A-horizons consisting of ash material and having the characteristics of a sandy loam texture. The soil profile of Nebrodi IV generally has a lighter colour, clay loam texture in the upper part and clay in the lowermost part of the profile. The soil profile Nebrodi IV had one distinctive argic horizon (Bt) with a high content of clays and a reddish-colour. The entire profile consists of five different parent materials, overshadowing any trend in chemical or physical constituents. In contrast to the Nebrodi profiles, the Sila profiles displayed a variety of brown colours and were shallower. In general, the soil thickness (A + B horizon) was between 90 and 160 cm at the Nebrodi sites and around 80 cm on the Sila mountains. In the topsoil, volcanic material was recognisable. The ash deposits at Nebrodi are sometimes > 100 cm thick (Fig. 3). The bulk density values in the upper part of the profiles were low, which is typical for soils having vitric properties (Table 3). According to the WRB (IUSS Working Group WRB, 2015), the diagnostic criteria for an andic horizon are: $Al_o + 1/2Fe_o > 2\%$, a bulk density < 0.9 g cm^{-3} and a phosphate retention ≥ 85%. The phosphate retention was not measured. The A and sometimes the B horizons often had a density below or close to 0.9 g cm^{-3}. Most of the samples did, however, not completely fulfil the criteria of $Al_o + 1/2Fe_o > 2\%$. Only the Nebrodi II profile and the Nebrodi IV profile (A2 horizon) met these requirements. Although the profiles contain a considerable amount of ashes and lapilli, several of them cannot be classified as Andosols. Except Nebrodi I, all other profiles in the Nebrodi mountains are composed of several substrates. Consequently, Fe_o and Al_o often strongly vary along the profiles.

Table 3
Physical characteristics of the investigated soils.

Site	Horizon	Depth (cm)	Munsell colour (moist)	Soil skeleton (wt%)	Bulk density (g/cm^3)	Sand (%)	Silt (%)	Clay (%)
Nebrodi I	A1	0–20	10YR1.7/1	0.9	0.84	34.8	44.7	20.5
	A2	20–50	10YR1.7/1	1.0	0.92	–	–	–
	A3	50–90	10YR1.7/1	0.7	0.93	–	–	–
	A4	90–130	10YR1.7/1	0.6	1.01	–	–	–
	AB	130–140	7.5YR3/1	0.6	1.49	68.3	16.6	15.1
	Bw	140–160	2.5Y5/6	0.6	1.58	57.0	18.9	24.1
Nebrodi II	A1	0–15	7.5YR3/1	1.3	1.00	41.7	27.7	30.6
	A2	15–50	7.5YR1.7/1	0.8	0.86	46.2	33.5	20.3
	2BA	50–65	7.5YR 4/4	19.2	0.89	55.0	30.4	14.6
	2Bw	65–90	7.5YR 4/4	49.3	0.74	59.0	29.6	11.4
	3BC	90–130	10YR 5/4	43.9	1.54	41.4	18.1	40.5
	4BC	130–170	10YR5/4	35.8	1.39	–	–	–
Nebrodi III	A1	0–50	10YR3/2	0.9	1.32	63.6	18.3	18.1
	A2	50–75	10YR1.7/1	4.3	0.98	–	–	–
	Bw	75–110	7.5YR4/3	17.6	1.27	69.5	20.6	9.9
	2BCg	110–135	10YR4/4	1.2	1.57	–	–	–
	2BC	135–155	10YR5/4	0.1	1.55	–	–	–
	3BC	155–170	10YR6/4	20.1	1.46	67.7	16.6	15.7
Nebrodi IV	A1	0–20	10YR2/1	5.0	0.80	36.6	33.5	29.9
	A2	20–35	10YR2/1	10.0	0.80	–	–	–
	2Btm	35–115	10YR3/6	10.0	0.90	54.0	31.0	15.0
	3Co	115–135	10YR3/4	40.0	1.10	–	–	–
	4Co	135–180	7.5YR4/4	35.0	1.10	–	–	–
	5Co	180–200	2.5Y4/4	10.0	1.25	–	–	–
	6C	> 200	2.5Y4/0	25.0	1.30	13.5	20.0	66.4
Sila I	A1	0–20	10YR3/4	2.0	0.87	37.1	38.0	24.9
	A2	20–40	10YR3/4	2.0	0.97	–	–	–
	Bw	40–60	10YR4/6	5.0	1.13	60.7	33.4	5.9
	2Bw	60–80	10YR6/4	5.0	1.37	–	–	–
	2C	80–100	10YR/6/3	10.0	1.37	70.9	22.4	6.7
Sila II	A1	0–20	10YR3/4	10.9	0.90	–	–	–
	A2	20–40	10YR3/4	15.1	0.83	–	–	–
	Bw	40–60	10YR4/6	15.8	1.11	–	–	–
	2Bw	60–80	10YR6/4	20.4	1.43	–	–	–
	2C	80–100	10YR/6/3	21.0	1.19	–	–	–

However, a maximum was measured in most cases in the B-horizon (Table 2). The majority of the soils at the Nebrodi sites had a pH-value (Table 2) of around 5 in the topsoil but showed a decrease of up to around 4 in the deeper B-horizons. This trend is most likely due to the ash input (unweathered fresh material) in the upper horizons giving rise to a higher pH. In the Sila mountains all the soils had a pH-value close to 5 with a tendency to increase with depth. In all the soils, organic carbon was found in most cases to a considerable depth. The organic C content, and therefore also the LOI, were particularly high in the soil Nebrodi I (Table 4). The thickness of the ash-bearing layer showed a considerable spatial variation at both mapped areas in the Nebrodi mountains, with 17 to > 100 cm close to Nebrodi II and 7 to > 100 cm close to Nebrodi III (Fig. 3).

3.2. Soil mineralogy

The DRIFT analysis (Table 5) of six soil profiles enabled the detection of a wide range of minerals that were confirmed by XRD analyses (Fig. 4). Kaolinite or halloysite (peaks at 3620 cm^{-1} and 3694 cm^{-1} in the IR spectra), gibbsite (at 3525 cm^{-1}), mica (given in the XRD spectra at 1.0 nm) and quartz (confirmed by XRD and the quartz doublet at 780 and 800 cm^{-1} in the IR spectra) were present in all profiles. In most profiles, a minor amount of smectitic phases (at 3624 cm^{-1}) seemed to be present. Typical for sediments and soils having a volcanic origin or input, a small amount of imogolite-type material (ITM: sum of imogolite and proto-imogolite allophane) was detected in many samples. Nebrodi IV, Sila I and Sila II showed also the presence of some amphibole in several horizons. Using XRD also iron oxides and traces of fayalite (olivine) were detected (Fig. 4).

3.3. Scanning electron microscopy data and related chemical analyses

The SEM-EDS analyses of thin sections enabled the detection of glass particles and volcanic clasts in all topsoil samples (Fig. 5). The glass particles often had small dimensions in the range of about 20–200 μm. They appear weathered at different extents (Fig. 5), showing coalescing etch pits and/or clay neogenesis (see Scarciglia et al., 2008). The main chemical composition of the site Sila (analysed on spots from better-preserved, fresh surfaces) appears quite homogeneous and has an essentially rhyolitic composition with a high silica (SiO$_2$ between about 75 and 78%) and alkali contents (Na$_2$O + K$_2$O between about 7 and 9%) and a TiO$_2$ content mostly in the range of 0.1–0.8% (Scarciglia et al., 2008; Vingiani et al., 2014). Using SEM-EDS, the samples of the Nebrodi site showed an average SiO$_2$ in the range of 62–72% and TiO$_2$ content of about 1.2% (0–2.7%).

LA-ICP-MS analyses were done on individual volcanic particles of the Nebrodi samples (Horizons A2 and A4 of Nebrodi I; A horizon of Nebrodi IV). Major and trace element contents are given in Table 6. Glasses, pumice-like material and volcanic clasts (sometimes considerably altered) were detected and measured (Fig. 5). Some samples analysed with SEM-EDS were re-measured. The more or less unweathered glass particles with minimal alteration have a quite uniform composition with a SiO$_2$ content of about 71–71 wt-% and a low TiO$_2$ content near 0.1 wt-%. The weathered volcanic clasts have, as an average, a lower SiO$_2$ (about 54–70 wt-%) and a higher TiO$_2$ content (0.2–1.1 wt-%). Some prominently vesicular (pumice-like) particles were also measured having a SiO$_2$ content of about 53 wt-% and TiO$_2$ of about 0.8 wt-%. The trace elements showed distinct variations among the distinguished material groups of the Nebrodi samples. Within the groups, the variability was limited suggesting a co-genetic link.

Table 4

Total elemental content (given as oxides) of all soil samples. LOI = loss on ignition; OM = organic matter, whereby the total organic C was determined via CHN-analyser and multiplied by the factor 1.72; IVC = inorganic volatile compounds, estimated by LOI minus OM.

Site	Horizon	Depth (cm)	Na$_2$O (g/kg)	MgO (g/kg)	Al$_2$O$_3$ (g/kg)	SiO$_2$ (g/kg)	P$_2$O$_5$ (g/kg)	K$_2$O (g/kg)	CaO (g/kg)	TiO$_2$ (g/kg)	MnO (g/kg)	Fe$_2$O$_3$ (g/kg)	LOI (g/kg)	OM (g/kg)	IVC (g/kg)
Nebrodi I	A1	0–20	19.2	13.7	169	490	6.5	19.1	16.7	10.1	1.7	58	196	189.1	7
	A2	20–50	18.8	13.7	184	522	6.3	20.1	14.4	10.7	1.8	60	148	162.1	0
	A3	50–90	18.0	13.6	184	526	6.3	19.8	14.5	10.6	1.8	59	146	124.6	22
	A4	90–130	20.5	14.5	191	524	6.6	19.9	15.8	10.9	1.8	60	135	124.7	10
	AB	130–140	17.8	19.2	195	649	2.0	27.1	12.2	6.6	0.8	37	33	16.3	17
	Bw	140–160	16.1	20.3	175	658	0.6	28.2	12.4	6.2	0.5	37	46	6.8	39
Nebrodi II	A1	0–15	14.7	15.9	168	566	3.6	20.2	19.4	9.0	1.8	57	124	82.7	42
	A2	15–50	14.9	13.1	191	491	5.7	17.4	17.8	10.7	2.0	66	170	113.4	57
	2BA	50–65	18.4	13.6	248	425	8.1	10.4	13.5	16.1	1.5	85	160	55.7	105
	2Bw	65–90	18.8	11.8	266	381	9.7	7.8	15.1	15.9	2.2	81	192	75.7	116
	3BC	90–130	8.6	10.3	100	764	0.5	13.8	4.5	4.6	1.5	42	51	5.4	45
	4BC	130–170	5.4	12.0	96	744	0.1	10.1	4.6	5.1	0.0	47	75	5.2	70
Nebrodi III	A1	0–50	19.8	16.4	164	673	1.4	27.7	8.9	5.4	0.7	31	52	32.9	19
	A2	50–75	18.5	15.0	211	542	4.8	21.8	9.2	10.0	1.2	56	110	69.1	41
	Bw	75–110	18.3	16.1	233	572	4.5	22.2	10.6	9.7	0.9	50	62	16.3	46
	2BCg	110–135	19.6	15.5	165	692	0.5	29.7	6.6	4.9	0.6	32	34	4.1	30
	2BC	135–155	16.6	17.5	166	692	0.5	30.3	7.2	4.6	0.5	30	35	4.7	30
	3BC	155–170	13.5	19.4	168	656	0.4	27.6	7.2	6.2	0.6	41	60	4.4	56
Nebrodi IV	A1	0–20	18.5	11.4	139	623	2.0	23.0	11.5	6.9	1.1	45	120	55.2	64
	A2	20–35	13.1	12.0	167	600	1.1	17.9	9.1	9.3	1.2	59	110	20.5	90
	2Btm	35–115	16.7	13.4	221	458	4.2	10.7	18.6	14.9	1.3	80	161	18.5	143
	3Co	115–135	26.1	14.8	238	447	6.8	9.0	34.1	15.5	2.0	83	124	9.7	115
	4Co	135–180	18.0	8.8	251	422	5.1	5.4	21.2	17.1	3.1	84	165	7.4	158
	5Co	180–200	13.7	10.6	123	710	0.1	19.8	7.5	6.2	1.8	44	63	2.6	61
	6C	> 200	4.3	9.4	86	732	0.1	11.7	3.9	4.8	0.1	66	82	5.8	76
Sila I	A1	0–20	18.3	11.3	191	508	2.4	23.8	19.8	7.1	0.8	49	168	100.8	67
	A2	20–40	17.6	11.4	199	528	2.2	25.3	21.1	7.1	0.8	50	137	67.3	69
	Bw	40–60	22.6	9.0	230	535	2.1	27.3	28.1	6.0	0.4	45	94	22.7	72
	2Bw	60–80	23.4	8.9	233	545	2.5	27.7	30.8	6.5	0.3	49	73	13.6	60
	2C	80–100	25.3	8.4	218	577	1.9	29.8	33.6	5.5	0.3	43	58	7.1	50
Sila II	A1	0–20	18.5	13.4	227	519	2.1	23.7	19.7	8.3	1.0	57	111	90.4	20
	A2	20–40	20.2	9.5	247	487	3.1	24.6	27.5	7.5	0.4	56	117	60.8	56
	Bw	40–60	26.7	8.9	239	530	2.7	25.1	35.2	6.1	0.3	46	80	33.4	47
	2Bw	60–80	33.7	9.7	254	543	2.9	24.7	36.9	5.9	0.3	45	44	8.9	35
	2C	80–100	26.9	8.8	247	542	3.0	25.5	37.6	6.1	0.3	44	58	9.2	49
Lapilli[a]	2BA	50–65	43.7	18.0	224	538	9.4	14.1	40.0	21.8	1.6	90	–	–	–
	2Bw	65–90	48.6	18.5	201	558	8.1	15.2	48.0	19.8	1.7	81	–	–	–
	2Bw	65–90	43.0	14.9	269	485	11.9	7.9	37.5	26.1	1.5	104	–	–	–
Arenite[b]			12.6	21.6	123	511	2.3	21.5	268.9	5.0	0.5	34	–	–	–

[a] Lapilli of the Nebrodi II site.
[b] Average composition of the arenite at the Monti Nebrodi sites.

3.4. Determination of the volcanic origin

Total alkali versus silica (TAS) diagrams are often used to determine the origin of igneous rocks and their extent of fractional crystallisation (Johannsen, 1937). However, the classical TAS diagram is not deemed suitable for determining the origin of unweathered rocks from bulk geochemical data of weathered soils, as enrichment and depletion of potassium or sodium in the soils, coupled with desilication, may have occurred. Weathering processes overshadow such a straightforward relation and may lead to potential errors. Instead, immobile or trace elements (Figs. 5 and 6) and their ratios including the Th-Co plot of Hastie et al. (2007) and the Nb/Y-Zr/Ti plot of Pearce (1996) were thus employed (Fig. 8a and b).

The source of the Sila volcanic material is not conclusive. The Hastie plots revealed the origin of a potassium rich calc-alkaline to shoshonitic origin for Sila I, Sila II and the extracted lapilli. Most samples of the Nebrodi sites can be characterised as trachy-andesite, whereas the Sila samples are related to the rhyolite/dacite domain. According to the Ti/Nb – Ti/Zr ratios (Fig. 6a), the Sila data showed a good agreement with the Roman Province, however this was not the case for any other chemical system (Figs. 6 and 7). Some overlap occurred with Campania (Figs. 6b, 7c) and Vultur (Fig. 6d). The most consistent trend was found for the Rb-Co (Fig. 6d), Zr/Rb – Th/Rb (Fig. 7b) and the K$_2$O/Na$_2$O – K$_2$O + Na$_2$O plots (Fig. 7a; Paterne et al., 1988) which suggest that the

Sila site is predominantly related to the Aeolian Islands.

The Nebrodi samples showed a clearer trend and this suggests sources from the Campania and Aeolian Islands domain as seen in the Ti/Nb-Ti/Zr (Fig. 6a), Sr-Rb (Fig. 7b) and Pb/Hf-Pb (Fig. 6c) plots. When looking at the Rb-Co (Fig. 6d), K$_2$O/Na$_2$O-K$_2$O + Na$_2$O (Fig. 7a; Paterne et al., 1988), Zr/Rb-Th/Rb (Fig. 7b) and Ce/TiO-TiO$_2$ (Fig. 7c) plots, the Nebrodi samples also exhibit a strong relation to the Aeolian Islands. In contrast, the lapilli collected at Nebrodi II were predominantly within the Sicily domain (Figs. 6 and 7; Paterne et al., 1988). A similar result was obtained for the lapilli using the Pb/Hf-Pb (Fig. 6c) and Zr/Rb-Th/Rb (Fig. 7b) diagram. The Lipari IIB event (epoch VI after Forni et al., 2013) and Vulcano events were closest to the soil data when using the Ce/Nd-Sr/Rb and Ce/La-Sr/Rb plots (Fig. 8c and d). In the Th-Th/U plot, the Lipari IIB event was even the only one that overlaps with the data of the soil samples (Fig. 8e).

All glasses showed similar levels of incompatible trace element enrichment reflected in their spidergrams and are up to > 800 times more enriched than in the primitive mantle. This enrichment is particularly given for Rb, Ba Th, and U. The profiles are characterised by a trough at Nb and Ta and a pronounced depletion in Ti (Fig. 5). The volcanic clasts, however, do not exhibit this Ti depletion. The glasses indicate a light rare earth element (LREE) enrichment relative to the heavy rare earth elements. Using the LA-ICP-MS analyses, the origin of the glass particles, pumice-like material and volcanic clasts can be fairly

Table 5
Identified minerals in the fraction < 32 μm using DRIFT.

Site	Horizon	Kaolinite	Gibbsite	Chlorite	ITM[a]	Illite (Mica)	Quartz	Smectite	Okt. (Mg/Fe)	AlMgOH	Amphibole
Nebrodi I	A1	x	x	?	(x)	x	x	(x)			x
	A2	x	x	(x)	(x)	x	x	(x)			
	A3	x	(x)			(x)	x	(x)			
	A4	x	?		(x)	x	x	(x)			
	AB	x	(x)		(x)	x	x	(x)			
	Bw	x	?				x				
Nebrodi II	A1	x	(x)		(x)	x		(x)		(x)	
	A2	x	x	(x)	(x)		x	(x)	(x)		
	2BA	?	x				x				
	2Bw	(x)	x	(x)	(x)	(x)	(x)	(x)		(x)	
	3BC	?	?		(x)		x	(x)			
	4BC	?	?		(x)	(x)	(x)	(x)			
Nebrodi III	A1	(x)	x		(x)	x	(x)	(x)		x	
	A2	x	x	?		x	x	x		(x)	
	Bw	x	x	x	(x)	x	x	(x)			
	2BCg	x	x	?	(x)	x	(x)			x	
	2BC	x	x	?	(x)	x	x	x		x	
	3BC	x	x		(x)	x	(x)	(x)	x	x	
Nebrodi IV	A1	x	?		?	x	x	(x)			x
	A2	x	?				x				x
	2Btm	x			(x)	(x)			(x)		
	3Co	?	x	?	?			x			x
	4Co	x	(x)		(x)	(x)	(x)				
	5Co	x	?		(x)		x				
	6C	(x)			(x)		x				
Sila I	A1	x	x	(x)	x	x	(x)		x	(x)	
	A2	x	x		x	(x)	(x)	(x)			(x)
	Bw	x	x		(x)	(x)	(x)	(x)			x
	2Bw	x	x	?	?						x
	2C	x	x		(x)	(x)					x
Sila II	A1	x	x	(x)	x	x	(x)		x	(x)	
	A2	x	x		x	(x)	(x)	(x)			(x)
	Bw	x	x		(x)	(x)	(x)	(x)			x
	2Bw	x	x	?	?						x
	2C	x	x		(x)	(x)					x

? = traces questionable, x = present in significant amount, (x) = low amount.
[a] ITM = imogolite-type material, henceforth referred to as the sum of imogolite and proto-imogolite allophane.
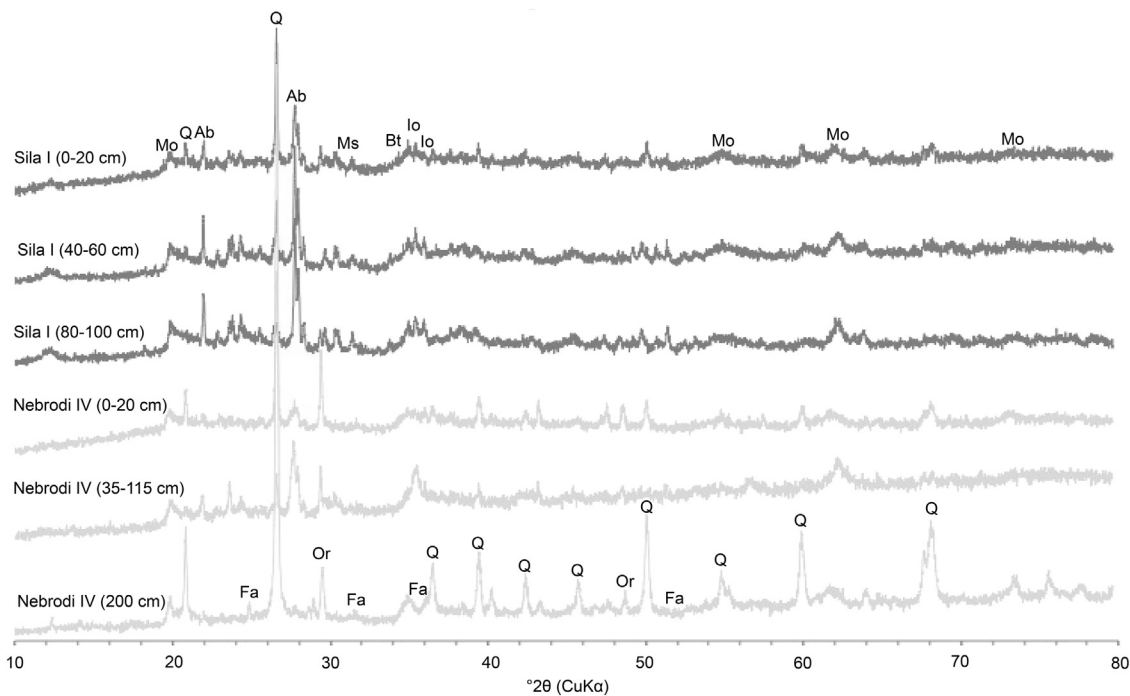
Fig. 4. X-ray diffraction patterns of six selected samples. Associated diffraction peaks are labelled as quartz (Q), albite (Ab), montmorillonite (Mo), iron oxide (Io), muscovite (Ms), biotite (Bt) and fayalite (Fa).
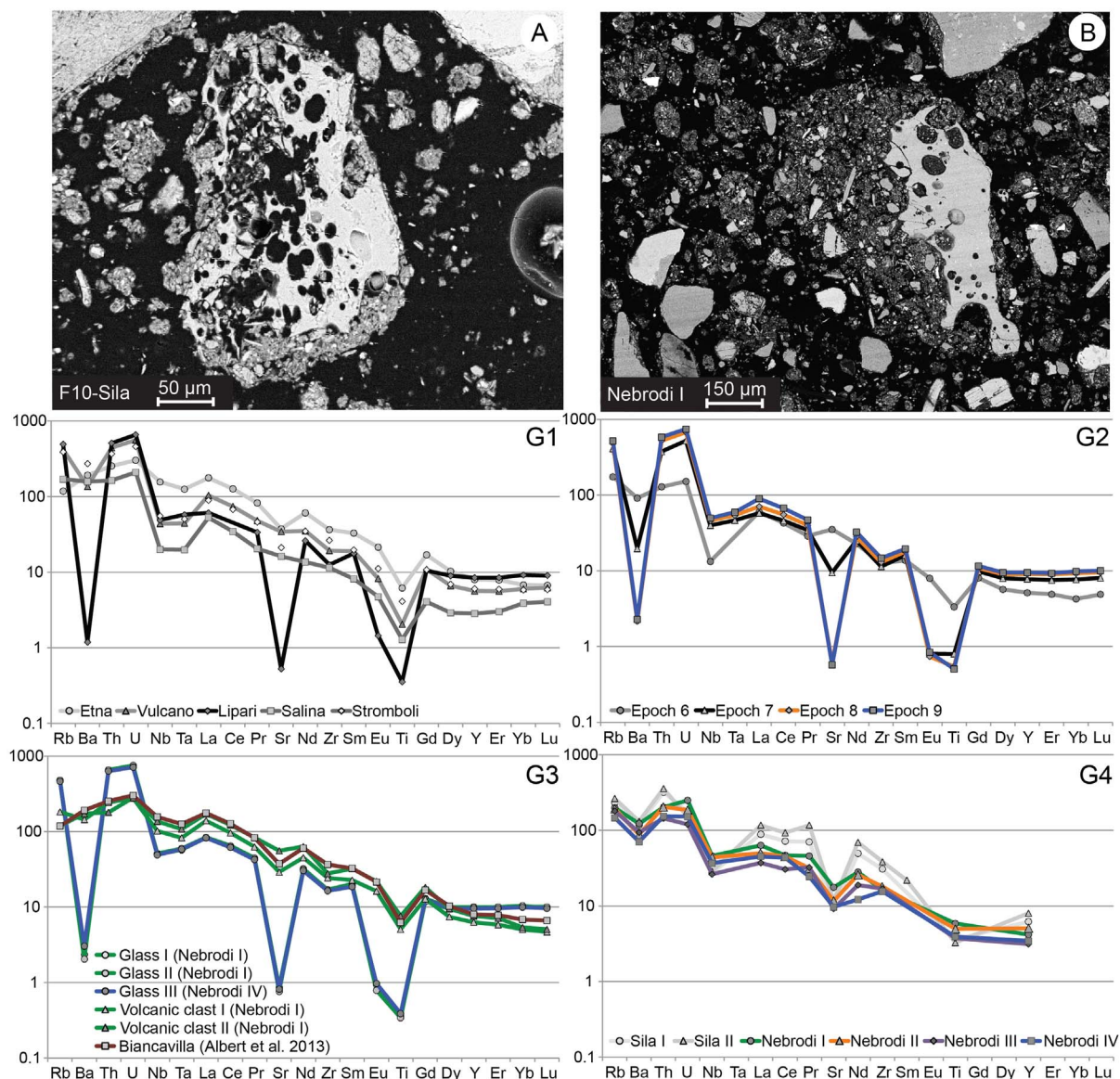
Fig. 5. SEM images of strongly weathered vesicular glass fragments of (A) Sila (Scarciglia et al., 2008) and (B) Nebrodi. Primitive mantle (Sun and McDonough, 1989) normalised data of G1) trace elements of volcanic glasses of the Aeolian Islands (Albert et al., 2017), G2) average composition of the Lipari volcanic epochs (Forni et al., 2013), G3) measured volcanic glasses and clasts in the Nebrodi soil profiles together with the Biancavilla deposits (Etna; Albert et al., 2013) and G4) average trace element composition of the investigated soil profiles.

well allocated by comparing them with data published by Forni (2011) and Albert et al. (2013, 2017). The glasses and clasts suggest an origin from the Aeolian Islands (although from different eruptive epochs) and the pumice-like material seems to fit well with a particular flank eruption of the Etna (the Biancavilla ignimbrites and Unit D Plinian fall deposits; Fig. 5).

3.5. Radiocarbon ages of OM

Age data of already published soil charcoal data are compiled in Table 7. The ages vary from modern to about 14 ka BP. Additional charcoal fragments, using the APOx preparation technique, did not result in higher ages (Table 7). Furthermore, nine soil samples were investigated (Table 8) that showed an overall age range from 319 to 9662 cal BP. The ages increased with soil depth at all sites. They showed that the oldest organic matter fractions that could be detected in the soils have a Holocene age. Maximum ages for the Nebrodi and Sila mountains from the H_2O_2-resistant soil organic matter fraction were in the range of 8–10 ka BP. The ages in the topsoil varied in the range of about 500–1800 ka BP at all sites.

3.6. Weathering indices

Weathering indices are given in Table 9. An undisturbed soil evolution would be characterised by increasingly weathered and leached horizons towards the surface. This is partially given for profile Nebrodi I. The sites Nebrodi II to IV however showed some discontinuities with less weathered material in the uppermost and lowermost horizons. Sila I and II had only little variation along the profile. The weathering indices used here do not always provide a conclusive signal where the (K + Ca)/Ti ratio indicates an increasingly weathered material towards the surface, while the CIW, CIA and PIA weathering indices showed less variations. In fact, these last three indices indicate less weathered material at the top and, thus, reflect the layering of the soil material. All weathering indices strongly correlated (highly significant; using the Spearman rank correlation) with each other. The weakest, but still highly significant correlation was between the (K + Ca)/Ti ratio and the index CIW ($R = 0.45$; $p < 0.01$) and the strongest between the index B and the CIA ($R = 0.999$; $p < 0.01$). In all these correlations, the 'bedrock' sample of the Nebrodi sites was an outlier.

Compared to the CIA, CIW and PIA indices, the WIP is known to

better cope with inhomogeneities in soils (Price and Velbel, 2003). Therefore, the WIP weathering index (using Fig. 9 as a basis) was used for an age estimate (Table 10). According to these estimates, the ash deposits in the Nebrodi mountains have an average age of about 70 ka and those in the Sila mountains about 49 ka (and 45 ka – with a considerable variability – when using the data of Scarciglia et al., 2008). The glass fragments found in the Sila soils would indicate even a lower age (between modern up to about 24 ka). Using the WIP, the volcanic deposits on the Nebrodi mountains seem to be older than those on the Sila mountains.

4. Discussion

4.1. Soil chemical and mineralogical properties indicate volcanic origin

The investigated regions of Nebrodi and Sila are considered to be suitable for distal tephra sedimentation due to their proximity to the Aeolian Arc and Mount Etna. Although the criteria for Andosols were not always fulfilled, andic-like and vitric properties could be observed in many places. Similar to other studies conducted on volcanic soils in southern Italy (Pichler, 1981; Pichler, 1984; Mirabella et al., 2005; Scarciglia et al., 2008; Egli et al., 2008; Vingiani et al., 2014), the total chemical composition of major and trace elements showed a dominance of SiO_2 and Al_2O_3 (Table 4). On average, the soils of the Nebrodi mountains had a slightly higher SiO_2 value (58.2%) compared to Sila area (53.0%). This is in agreement with the values reported in Scarciglia et al. (2008) and Vingiani et al. (2014). Kaolinite or halloysite were commonly found in all the investigated soils. Kaolinite and halloysite are typically found in volcanic soils and were presumably formed through the weathering sequence: glass > halloysite > kaolinite (Mirabella et al., 2005; Egli et al., 2008). Gibbsite is similarly produced by chemical weathering of aluminium-rich rocks (Glenn and Nash, 1964). Smectite-like clay minerals were also found, particularly in the A-horizon. According to Sumner (1999), Mirabella et al. (2005), Egli et al. (2008) and De Rosa et al. (2016), smectite is often found in volcanic soils, possibly created through hydrothermal processes. The DRIFT analysis also revealed the presence of imogolite (typically in the A and B horizons) — a typical short-range order (poorly crystalline) mineral found in volcanic soils that were formed from ashes/tephra (Sumner, 1999). The clay assemblages confirms the volcanic origin of the soils.

4.2. Origin of the volcanic deposits

Given the locations of Nebrodi and Sila, several volcanic areas (Fig. 7d) could potentially contribute volcanic material to the soils. The main challenge in determining the origin of these deposits is to find a method that can differentiate the volcanoes from each other while excluding influences due to alteration. The chemical composition of the soils and of the potential volcanic sources (Pichler, 1967; Scarciglia et al., 2008; Pelle et al., 2013; Vingiani et al., 2014) can be used for a forensic analysis especially the element ratios Th/Rb vs Zr/Rb, TiO_2 vs Ce/TiO_2 and K_2O/Na_2O vs K_2O + Na_2O were useful for alteration material. We also considered currently inactive volcanic systems (e.g. only Etna and Stromboli are presently active). Th-Co (Hastie et al., 2007) is unaffected by the enrichment and depletion of potassium or sodium in soils, making it a good indicator of the geochemistry of the original source. All the soils investigated here fall into the high-K calc-alkaline series (Fig. 8a; Peccerillo, 2005). This allowed us to exclude several volcanic centers based on their petrochemical affinity, such as Na-alkaline and transitional series (Sardinia, Sicily, Sicily Channel), crustal anatectic (Elba, Giglio), K-alkaline (Tuscany, Umbria, Ernici-Roccamonfina, Vultur) and tholeiitic (Montiferro) sources. Only the Aeolian Arc, Roman Province and part of Campania in southern Italy display similar geochemistry (Keller et al., 1978; Pichler, 1981; Paterne et al., 1988; Narcisi and Vezzoli, 1999; Peccerillo, 2005; Forni, 2011;

Albert et al., 2017). Mount Etna was initially assumed to be a major source due to its close proximity to the research areas and its enormous eruption rates during the past four centuries (Condomines and Tanguy, 1995). However, while the lapilli layers do seem to be derived from Etna (Figs. 5 and 6), the generally alkaline to tholeiitic series volcanism (Peccerillo, 2005) does not fit with the rest of the soil data (Fig. 8a). Albert et al. (2013) analysed volcanic glasses from the Biancavilla ignimbrites and Unit D Plinian fall deposits of Mt. Etna. These deposits can be ascribed to the explosive activity (about 17–19 ka BP) within the predominantly effusive and mildly explosive (Strombolian) volcanic history of Mount Etna. The explosive eruptions from Etna are considered responsible for widespread ash dispersals throughout the central Mediterranean region, producing marker tephra layers. Compared to other eruptions from Mt. Etna, the chemical composition of the Biancavilla ignimbrites is more evolved and acidic. The Biancavilla ignimbrites and Unit D Plinian fall deposits have a SiO_2 content in the range of about 60–64% and a Na_2O + K_2O content in the range of 8.9–9.9% (Albert et al., 2013). According to our LA-ICP-MS analyses, part of the volcanic particles (pumice) can be most likely ascribed to this Biancavilla ignimbrites and Plinian eruptions. Mt. Etna therefore has contributed to the volcanic deposits of the Nebrodi mountains and maybe also to the deposits in the Sila mountains.

The high-K calc-alkaline to shoshonite series composition of the soils (Fig. 8a) are, however, also typical for island arcs and subduction magmatism (Joplin, 1968; Morrison, 1980; Pichler, 1981) and match Campania and Aeolian Arc volcanism. This is demonstrated in the Ti/ Nb – Ti/Zr, Rb-Co, Ce/TiO_2 – TiO_2 plots (Fig. 6a and d and Fig. 7c). Zr/ Rb versus Th/Rb and K_2O/Na_2O versus K_2O + Na_2O (Fig. 7a; Paterne et al., 1988) also indicate that the soils of Nebrodi and Sila were strongly affected by the Aeolian Arc during their pedogenesis. This agrees well with Scarciglia et al. (2008) who suggested that the volcanic ash fragments of the Sila uplands derive from the Aeolian Arc, particularly from Lipari as the main source. However, as described above, the chemistry of the lapilli strongly differs from the soil (Table 4). The analysed lapilli fragments found in the soil of Nebrodi II appear to derive from Sicily (Fig. 6a–d and Fig. 7a, c) suggesting input from Mount Etna. In a next step, a discrimination between the different volcanoes of the Aeolian Arc was undertaken.

According to Pichler (1967), the volcanic archipelago of the seven Aeolian Islands has always been separated into two groups based on their chemical composition. The first group (A) consists of the islands of Lipari, Salina, Filicudi, Alicudi and Panarea-Basiluzzo, while the other (B) includes the islands of Vulcano and Stromboli. Group A is characterised by a normal-calk-alkaline magma, except for the high-K calc-alkaline (to shoshonitic) volcanic activity epochs II, V, VI and VII (Fig. 10) of Lipari (Pichler, 1981; Forni et al., 2013). Group B has a potassium-rich calk-alkaline magma development (Pichler, 1981). According to several studies (e.g. Joplin, 1968; Munno et al., 1980; Pichler, 1981; Bertagnini et al., 2008), the islands Stromboli and Vulcano clearly differentiate themselves from the rest of the Aeolian volcanoes due to their strong shoshonitic signatures (Joplin, 1968; Bertagnini et al., 2008; De Astis et al., 2013; Francalanci et al., 2013). Shoshonites are basaltic rocks rich in potassium and classified as trachy-andesite (Joplin, 1968; Munno et al., 1980; Pichler, 1981). The majority of the Nebrodi samples fit the field of trachy-andesite. This is in contrast to the Sila samples that seem to be related to the rhyolite/dacite field (Fig. 8b). Dacite and andesite rocks are typical for the epochs IV, V and VI, whereas the epochs VII–IX of Lipari are dominated by dacite to rhyolite effusive rocks (Forni et al., 2013). The eruptive history of Vulcano predominantly consists of shoshonites, basalts and a minor amount of trachyte (-andesite) (De Astis et al., 2013). From a forensic point of view, the most likely volcanic sources of the investigated samples are several epochs of Lipari and Vulcano. Based on the data of Pichler (1984), the investigated samples are chemically close to Vulcano and Lipari phase IIB and the epochs V and VI of Lipari (Fig. 10; Forni et al., 2013). Taking into account that the Nebrodi samples even

Table 6
Major, minor and trace elements data measured by LA-ICP-MS on glass shards from Nebrodi soil samples.

Profile	Nebrodi I			Nebrodi I	Nebrodi IV	
Horizon	A2 (20–50 cm)			A4 (90–130 cm)	A1 (0–20 cm)	
Material	Glass I (n = 5)	Glass II (n = 3)	Volcanic clast I (n = 2)	Volcanic clast II (n = 6)	Glass III (n = 3)	Pumice I (n = 2)
Major elements (wt-%)						
SiO$_2$	71.17 ± 0.16	72.20 ± 0.07	54.86 ± 1.55	54.00 ± 1.78	72.03 ± 0.85	52.48 ± 4.28
TiO$_2$	0.08 ± 0.00	0.07 ± 0.00	1.10 ± 0.03	1.65 ± 0.22	0.08 ± 0.01	0.81 ± 0.07
Al$_2$O$_3$	13.82 ± 0.16	13.34 ± 0.10	22.11 ± 3.54	15.9 ± 1.61	13.53 ± 0.39	23.41 ± 2.15
FeO	1.64 ± 0.10	1.54 ± 0.01	7.10 ± 3.07	7.70 ± 1.33	1.61 ± 0.03	9.57 ± 0.05
MnO	0.07 ± 0.00	0.06 ± 0.00	0.21 ± 0.15	0.17 ± 0.05	0.07 ± 0.01	0.26 ± 0.02
MgO	0.04 ± 0.00	0.04 ± 0.00	1.68 ± 0.17	2.70 ± 1.00	0.06 ± 0.02	2.63 ± 0.01
CaO	0.81 ± 0.05	0.75 ± 0.03	2.81 ± 1.95	6.83 ± 1.86	0.74 ± 0.06	4.66 ± 2.09
Na$_2$O	4.36 ± 0.01	4.07 ± 0.04	4.24 ± 2.86	4.75 ± 0.58	4.03 ± 0.23	0.54 ± 0.02
K$_2$O	5.02 ± 0.11	4.92 ± 0.10	2.88 ± 0.61	3.29 ± 0.47	4.83 ± 0.24	2.63 ± 0.12
Total	97.0	97.0	97.0	97.0	97.0	97.0
Trace elements (μg/g)						
V	0.9 ± 0.31	0.6 ± 0.03	128.0 ± 84.70	237.1 ± 58.08	2.9 ± 2.53	179.9 ± 3.4
Co	0.4 ± 0.09	0.3 ± 0.05	15.8 ± 11.97	18.1 ± 2.95	0.9 ± 0.77	21.5 ± 0.8
Rb	302.5 ± 8.27	304.4 ± 2.59	116.5 ± 59.12	75.7 ± 11.56	293.4 ± 13.85	227.7 ± 12.9
Sr	18.3 ± 1.93	16.0 ± 0.15	614.8 ± 354.51	1179.7 ± 127.62	17.2 ± 0.54	262.8 ± 83.1
Y	45.6 ± 0.71	45.1 ± 0.61	28.7 ± 0.42	34.8 ± 8.87	43.5 ± 1.35	153.4 ± 77.4
Zr	189.6 ± 1.50	187.2 ± 3.26	272.6 ± 131.10	310.5 ± 36.85	183.0 ± 5.93	112.3 ± 9.6
Nb	36.5 ± 0.71	35.7 ± 0.73	72.7 ± 33.56	97.1 ± 18.01	34.9 ± 0.11	34.7 ± 2.5
Cs	16.9 ± 0.48	17.1 ± 0.25	5.2 ± 6.23	1.8 ± 0.22	16.6 ± 0.60	10.0 ± 1.3
Ba	16.6 ± 1.01	14.3 ± 0.15	1009.1 ± 430.13	1214.0 ± 186.90	21.1 ± 5.93	606.7 ± 76.3
La	58.0 ± 0.61	57.2 ± 0.47	95.5 ± 4.99	117.9 ± 17.56	56.7 ± 1.76	442.8 ± 233.9
Ce	115.1 ± 2.77	111.4 ± 0.71	171.1 ± 5.75	217.9 ± 41.85	109.4 ± 3.61	391.1 ± 173.8
Pr	12.3 ± 0.34	12.0 ± 0.20	17.3 ± 0.62	23.0 ± 4.78	11.7 ± 0.31	72.4 ± 35.8
Nd	43.5 ± 0.84	42.3 ± 0.33	61.2 ± 2.70	86.0 ± 18.84	40.9 ± 2.03	257.0 ± 128.6
Sm	9.0 ± 0.13	8.5 ± 0.36	10.2 ± 0.27	14.4 ± 3.67	8.3 ± 0.82	45.0 ± 22.1
Eu	0.2 ± 0.01	0.1 ± 0.03	2.7 ± 0.52	3.7 ± 0.32	0.2 ± 0.04	10.6 ± 5.9
Gd	7.7 ± 0.11	7.1 ± 0.15	7.7 ± 0.17	10.9 ± 2.86	7.5 ± 0.69	38.2 ± 18.8
Tb	1.1 ± 0.03	1.1 ± 0.02	1.0 ± 0.01	1.3 ± 0.32	1.1 ± 0.15	5.0 ± 2.8
Dy	7.4 ± 0.20	7.0 ± 0.21	5.5 ± 0.01	7.0 ± 1.97	7.0 ± 0.10	24.9 ± 11.4
Ho	1.5 ± 0.03	1.4 ± 0.08	1.0 ± 0.03	1.3 ± 0.34	1.5 ± 0.04	4.2 ± 2.0
Er	4.8 ± 0.09	4.8 ± 0.22	2.8 ± 0.12	3.4 ± 1.11	4.7 ± 0.24	10.8 ± 5.3
Tm	0.7 ± 0.02	0.7 ± 0.02	0.4 ± 0.02	0.4 ± 0.12	0.7 ± 0.02	1.3 ± 0.6
Yb	5.0 ± 0.18	5.1 ± 0.27	2.5 ± 0.10	2.6 ± 0.65	4.9 ± 0.13	7.7 ± 3.6
Lu	0.7 ± 0.02	0.7 ± 0.04	0.3 ± 0.00	0.4 ± 0.10	0.7 ± 0.01	1.1 ± 0.4
Hf	6.7 ± 0.07	6.8 ± 0.27	5.6 ± 2.21	6.2 ± 1.01	6.6 ± 0.47	2.3 ± 0.3
Ta	2.4 ± 0.01	2.3 ± 0.07	3.4 ± 1.62	4.4 ± 0.78	2.4 ± 0.05	1.5 ± 0.2
Pb	30.8 ± 1.48	32.3 ± 2.61	43.6 ± 41.73	17.4 ± 0.70	30.2 ± 0.62	76.2 ± 16.3
Th	55.7 ± 0.25	54.0 ± 0.41	20.6 ± 1.14	15.3 ± 1.19	53.9 ± 1.75	18.4 ± 5.1
U	15.9 ± 0.44	15.1 ± 0.27	5.9 ± 0.73	5.9 ± 0.86	15.0 ± 0.19	9.5 ± 3.8

showed a stronger inclination to Lipari using the Th – Th/U plot (Fig. 8e), we suggest that Lipari is the main source for both sites.

Several horizons seemed to be purely composed of volcanic material while some were a mixture (volcanic material mixed with the in situ parent material). Given a known 'parent material' at the sites of interest, the proportion of volcanic material in the soils of Nebrodi and Sila can be roughly estimated. Having a mixture of two different materials, their proportion can be estimated by using inert components under the prevailing weathering conditions (Sommer et al., 2000). Based on the available data and using the concept of weathering indices, Al$_2$O$_3$ and TiO$_2$ were used as tracers. Using a mass balance approach, we have:

$$a\mathrm{Al_2O_3(pm)} + b\mathrm{Al_2O_3(v)} = c\mathrm{Al_2O_3(fe)} \quad (7)$$

$$a\mathrm{TiO_2(pm)} + b\mathrm{TiO_2(v)} = c\mathrm{TiO_2(fe)} \quad (8)$$

$$a + b = 1 \quad (9)$$

where a is the relative proportion of the parent material and b is the relative proportion of the volcanic source (Aeolian Islands; Lipari; data from Mirabella et al., 2005 and Peccerillo, 2005). The letter c denotes the weathering coefficient of the soil; Al$_2$O$_3$(pm), Al$_2$O$_3$(v), TiO$_2$(pm) and TiO$_2$(v) are the contents of the parent material (*pm*) and volcanic source (*v*). Al$_2$O$_3$(fe) and TiO$_2$(fe) are the contents in the fine earth of

the soil. Solving the three linear equations with three unknown results in (Sommer et al., 2000):

$$c = \frac{\mathrm{TiO_2(v)[Al_2O_3(pm) - Al_2O_3(v)] - Al_2O_3(v)[TiO_2(pm) - TiO_2(v)]}}{\mathrm{TiO_2(fe)[Al_2O_3(pm) - Al_2O_3(v)] - Al_2O_3(fe)[TiO_2(pm) - TiO_2(v)]}} \quad (10)$$

and

$$a = \frac{c\mathrm{Al_2O_3(fe) - Al_2O_3(v)}}{\mathrm{Al_2O_3(pm) - Al_2O_3(v)}} \quad (11)$$

Due to the high heterogeneity of the soils, it is difficult to assign a single parent material: in the case of Nebrodi II, four different substrates along the profile were defined and for Nebrodi IV even six (Tables 2 and 4; Fig. 2d). In such cases, we assumed that the horizon directly underlying the ash is indicative of the 'parent material' (the likelihood seems to be greatest that ash deposits were mixed with this layer). In several cases (Table 11), the source material of the topsoil and parts of the subsoil seem to originate up to 100% from Lipari. In general, the proportion of ash increases towards the surface, matching the macromophological examinations (Fig. 2). In addition, we also calculated the proportion of the Biancavilla ignimbrites and Unit D Plinian fall deposits on the soil composition (A horizons). Compared to Lipari, the geochemical overlap of the Biancavilla eruptions with the
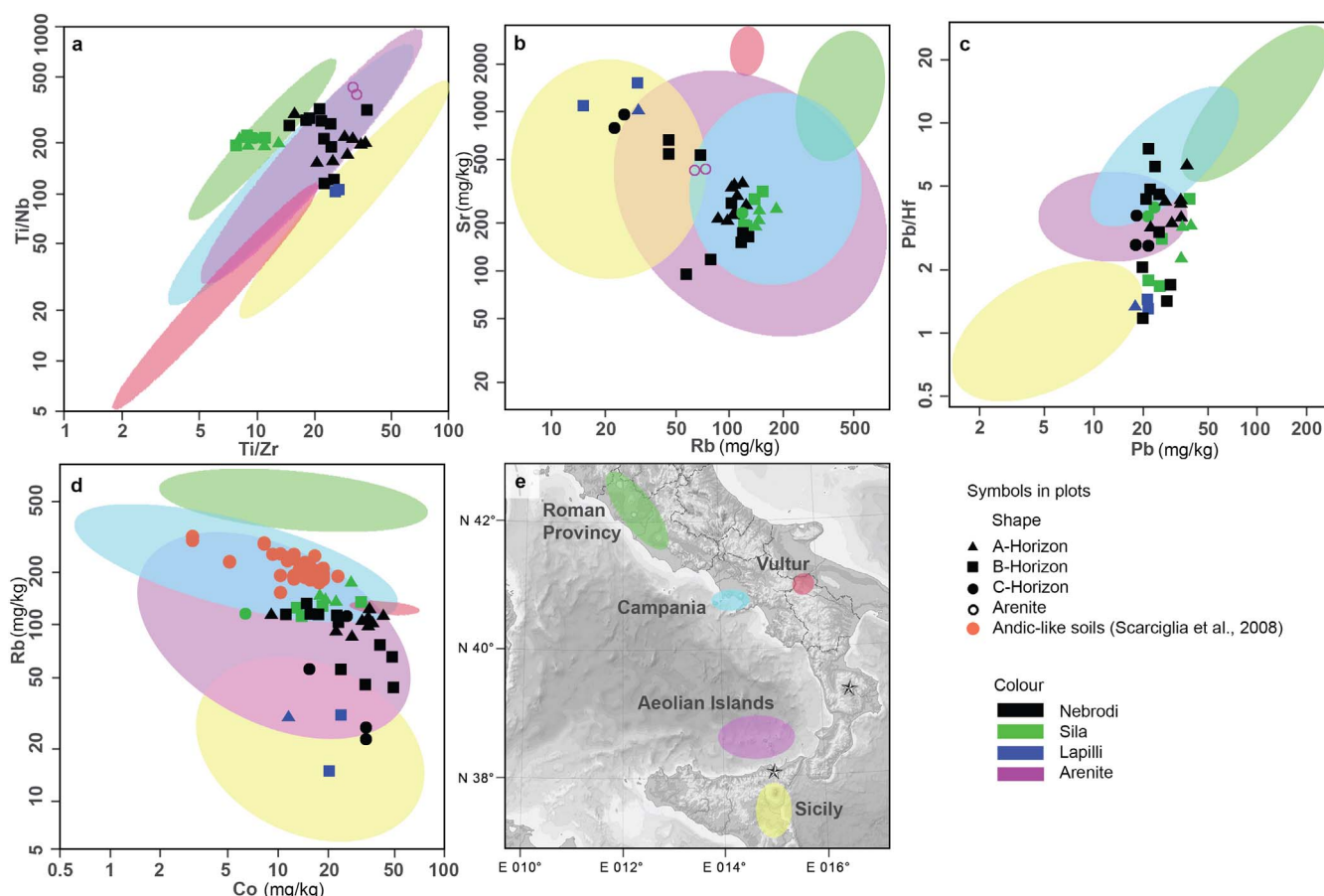
Fig. 6. Geochemical forensics based on a comparison between the a) Ti/Nb-ratio and Ti/Zr-ratio, b) Sr vs Rb, c) Pb/Hf-ratio vs Pb and d) Rb vs Co. e) The coloured fields are used as a reference for the corresponding volcanic areas based on data of Peccerillo (2005). The two stars mark the locations of the investigation sites Nebrodi and Sila mountains. In addition, the values given in Scarciglia et al. (2008) are also plotted. (For interpretation of the references to colour in this figure legend, the reader is referred to the web version of this article.)

investigated soils is small. At some sites, the Biancavilla ignimbrites and Unit D Plinian fall deposits may explain up to 80% of the main geochemical composition, while at other sites they are absent. The explanatory power of the Biancavilla ignimbrites and Unit D Plinian fall deposits on the geochemical composition of the soils seems therefore lower compared to the Lipari effusiva. It is, however, still very likely that the Biancavilla and Plinian eruptions have contributed (to a smaller extent) to the volcanic deposits on the Sila and Nebrodi mountains. Due to bioturbation, erosion and chemical weathering, such volcanic deposits are partially mixed with older volcanic deposits. It seems that the predominant source of volcanogenic material are the Aeolian Islands with some contributions from the Etna.

4.3. Age estimates from weathering indices

Scarciglia et al. (2008) estimated the age of the volcanic deposits in the Sila mountains (start of formation of ando-like soils) by radiocarbon dating charcoal. Three charcoal fragments were taken from mineral horizons of three different soil profiles (samples from a surface horizon, a buried horizon and from a subsurface horizon), yielding ages between 3383–3355 to 254–33 ka cal BP (Table 7). However, clay coatings found in the ando-like soil horizons together with their stratigraphic position overlying a rubified soil of the last Interglacial imply an older, not clearly defined time range, from the Late Pleistocene to the Holocene. Based on this, the authors hypothesised that the volcanic ash contributions probably derived from the Aeolian Arc explosive activity spanning the last 30 ka. Pelle et al. (2013) refined this interpretation, suggesting a slightly older input of pyroclastics dating back to the last 42 ka.

Our approach, by using the H_2O_2-resistant organic matter fraction as an approximate indicator for the start of soil formation (Favilli et al., 2009a, 2009b) gave an age of about 8.2 ka cal BP for the Sila volcanic ash deposits and about 9.6 ka cal BP for the Nebrodi ash deposits (Table 8). The $\delta^{13}C$ values of the H_2O_2-resistant carbon indicate in most cases C4 plants, except for Nebrodi I and III. This might be due either to a fractionation during adsorption or due to a former cultivation with C3 plants which has been quite common in Sicily since the Islamic period (Egli et al., 2013). While older than the radiocarbon data (3.1 ka BP) of Scarciglia et al. (2008) and estimates from archaeological finds in the same soils ($\leq$ ca. 5.8 ka BP; Pelle et al., 2013), our H_2O_2-resistant radiocarbon results still indicate a purely Holocene age (Table 8). Recent charcoal dating in these soils has yielded ages of up to 5 ka in the A horizon and up to about 14 ka cal BP in the underlying B horizon (Moser et al., 2017; Table 7), hinting again that the ash deposits must already have been present in the Late Pleistocene. In general, ^{14}C-ages of charcoal increased with increasing depth due to bioturbation, transport in macropores and accumulation of aeolian deposits on top. Remote aeolian transport of macrocharcoal can be usually excluded (Carcaillet and Brun, 2000; Lynch et al., 2004; Favilli et al., 2010).

To help refine the chronology of these soils, we also estimated the age of the volcanic deposits using an empirical relation to the WIP weathering indices (Fig. 9). These ages could then be correlated to the activity phases of the volcanoes of the Aeolian Arc (Fig. 10). Compared to other weathering indices, the WIP better copes with inhomogeneities of the samples (Price and Velbel, 2003). Soil genesis on the Sila mountains started between 45–49 ka BP based on WIP-derived ages and seems to have been influenced by the Aeolian Arc explosive activities (Table 10) over at least the last about 50 ka (Table 11). This fits nicely
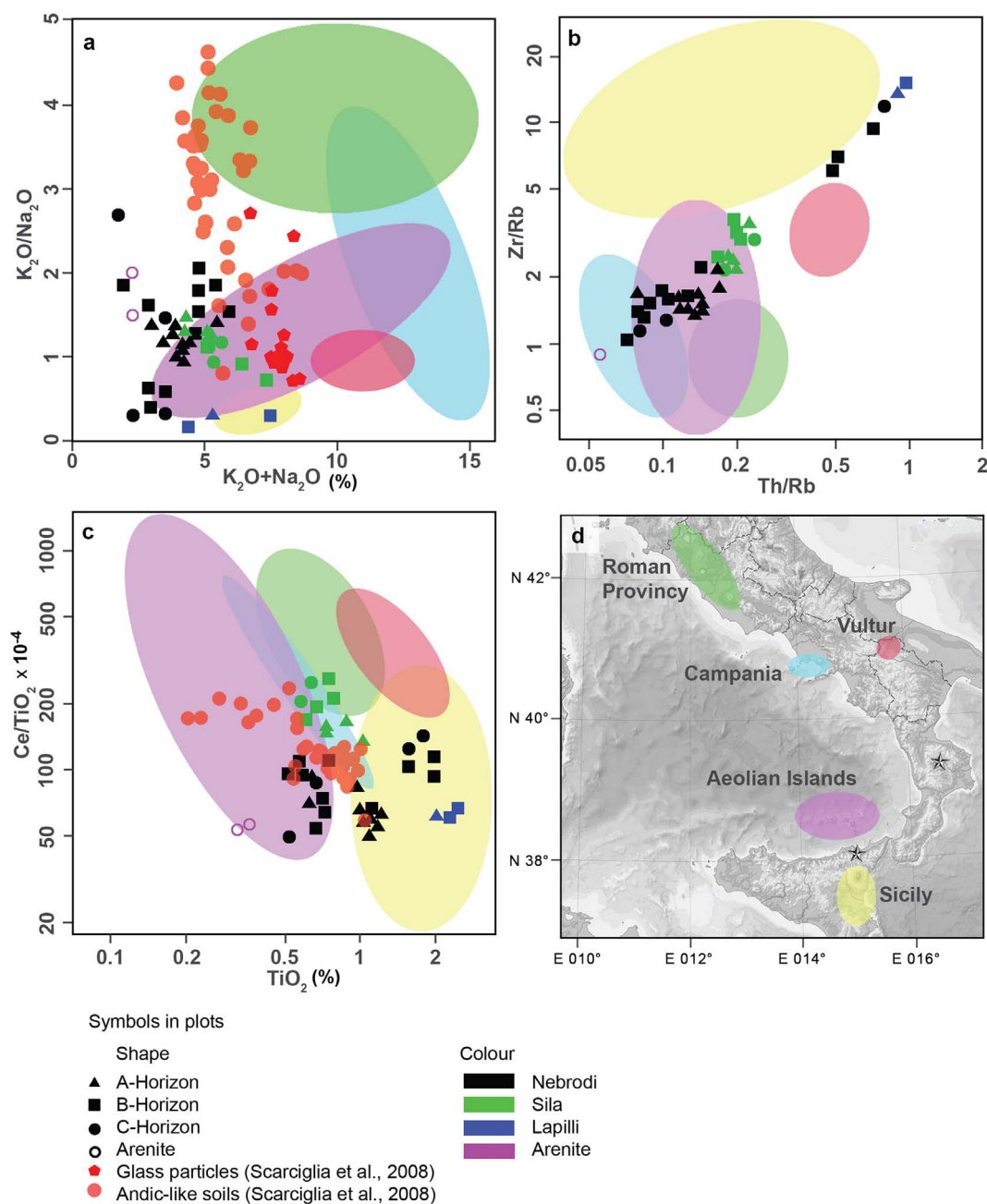
Fig. 7. Geochemical forensics based on a comparison between a) the alkali ratio (K_2O/Na_2O) vs total alkali diagram ($K_2O + Na_2O$) according to Paterne et al. (1988), b) Zr/Rb- vs Th/Rb-ratio and c) Ce/TiO_2-ratio vs TiO_2. d) The coloured fields are used as a reference for the corresponding volcanic areas based on data of Peccerillo (2005). The two stars mark the locations of the investigation sites Nebrodi and Sila mountains. In addition, the values given in Scarciglia et al. (2008) are also plotted. (For interpretation of the references to colour in this figure legend, the reader is referred to the web version of this article.)

with the first estimates done by Scarciglia et al. (2008) and Pelle et al. (2013). On the Nebrodi mountains, the influence of the Aeolian Arc seems to have started even earlier (70 ka BP). The geochemistry (major and trace elements) of volcanic clasts (Table 6), furthermore, fits best with the eruption epoch 6 of Lipari (mostly between 81 and 92 ky BP; Forni, 2011). The glass components in the soils seem to have a younger age and fit nicely with the eruption epochs 7–9 (< 70–1 ka BP). The pumice-like components can be attributed to the Biancavilla and Plinian eruptions (ca. 17–19 ka BP; Albert et al., 2013).

The apparent inconsistencies between the radiocarbon dates and geochemical indices-estimated ages can have several reasons. It seems that a considerable part of the volcanic deposits has its origin in older eruptive epochs of the Pleistocene (roughly between 80 and 90 ka PB; Table 10). Between the Late Pleistocene and Holocene, several

additional eruptive epochs of the Aeolian Islands (epochs 7–9, according to Forni, 2011) and Etna (particularly the Biancavilla and Plinian eruptions; Albert et al., 2013) have occurred. The dated charcoal pieces fall into this second period. Charcoal and soil organic matter of the earlier phase was most likely not conserved (it furthermore would be out of the dating range of ^{14}C). The fate of soil organic matter also depends on the strong chemical interactions during weathering. Decay of soil organic matter on 10 ka timescales or mineral transformation and surface properties changes may have released strongly bound organic phases (Torn et al., 1997; Kleber et al., 2007). It is, furthermore, likely that macro-charcoal is not that stable in these environments (only very few samples had an age of > 8 ka; Moser et al., 2017; Table 7). This is probably related to a bad preservation of charcoal. De Lafontaine et al. (2011) suggested that the permineralization process increases the
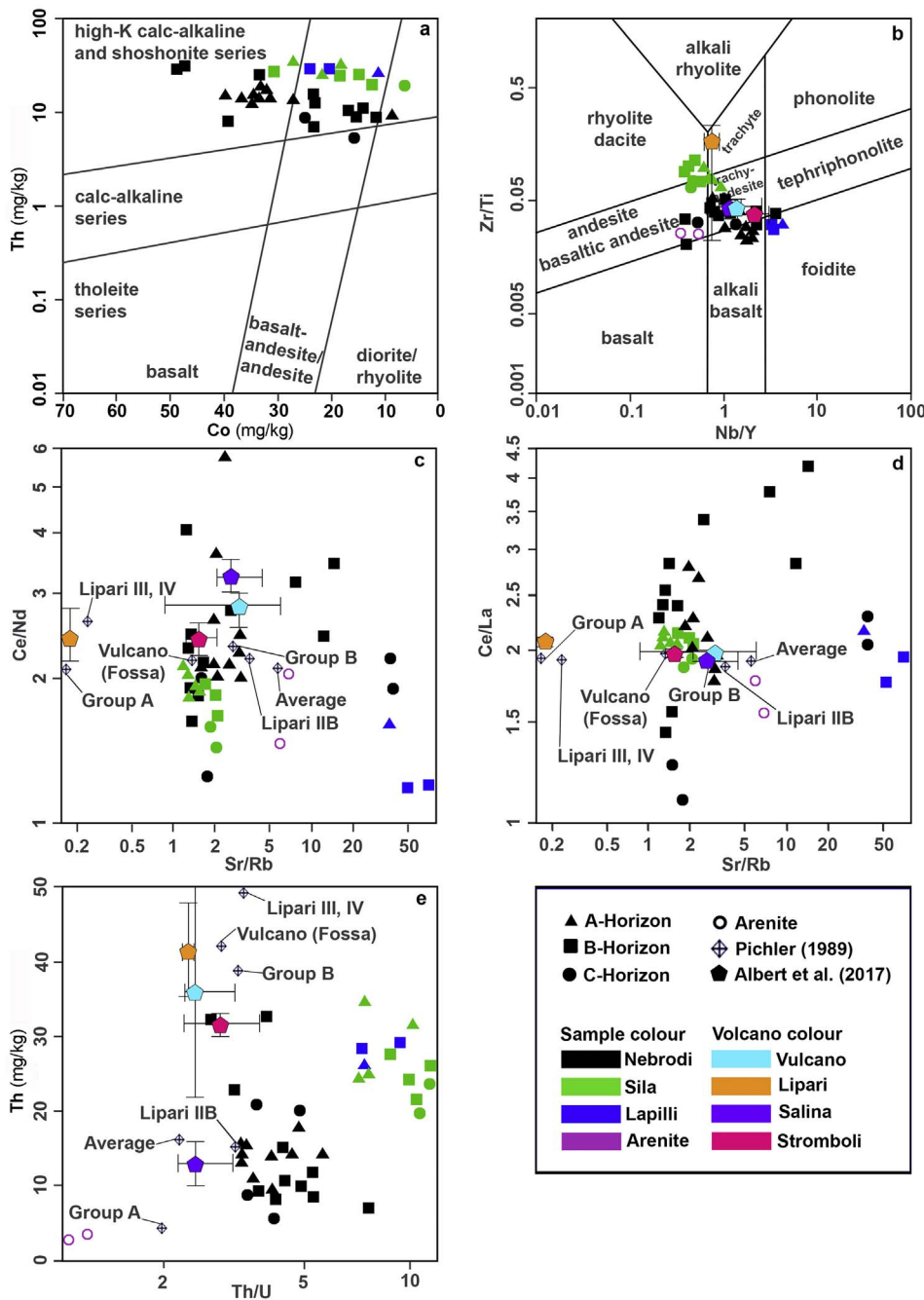
Fig. 8. Geochemical forensics based on a) the Co-Th plot after Hastie et al. (2007), b) Zr/Ti-ratio against Nb/Y-ratio plot after Pearce (1996), c) and d) Ce/Nd-ratio and Ce/La-ratio vs the Sr/Rb-ratio and e) Th vs Th/U-ratio. Group A includes the Aeolian Islands Lipari, Salina, Fillicudi, Alicudi, Panare-Basiluzzo and Group B Lipari IB, III, IV (equals the epochs I, VIII and IX after Forni et al. (2013)), Vulcano and Stromboli (Pichler, 1989).

density of charcoal particles and thus offers a protection against subsequent degradation. This fossilisation process consists in concealing wood structures by massive mineral filling inside the cavities. Charcoal fragments are, furthermore, well preserved in acidic environments (Weiner et al., 1993; Karkanas et al., 2000). Under only slightly acidic conditions (as at the investigation sites), the preservation is therefore not optimal.

By cross-referencing the estimated time windows based on the WIP, the calculated ages would fit best with the eruption epochs of Vulcano, Lipari and Alicudi (Fig. 10), and partially with Stromboli. Forni et al. (2013) described the epoch V of Lipari as recurrent hydromagmatic explosions and the epoch VI of Lipari as Vulcanian-type explosive phases. De Astis et al. (2013) stated that the eruptions of epoch III of Vulcano were effusive and coupled with a hydromagmatic phase. All of these epochs had a high-K calc-alkaline volcanism, although Vulcano had a tendency towards a shoshonite composition (De Astis et al., 2013;

Forni et al., 2013). Based on these findings, the epochs VI–IX of Lipari were probably the main sources for the Sila soils with the epoch VI of Lipari together with some input of the Etna influencing Nebrodi. Volcanism from Vulcano cannot be fully excluded from having contributed to the volcanic deposits of the study areas.

5. Conclusions

Using a multi-method approach, the origin and age of soils formed from volcanic deposits in southern Italy could be tentatively determined. When comparing soil material with volcanic deposits, the main geochemical composition may be used as a forensic indicator. However, due to weathering and leaching processes, the composition of soils might be altered. It is therefore strongly recommended to use alternative tracers for determining the origin of volcanic deposits such as relatively 'immobile' elements and their ratios among each other (e.g.

Table 7

Radiocarbon dates of charcoal found in the soils of the Sila highland. Datasets are from Moser et al. (2017), Scarciglia et al. (2008) and new measurements.

Soil profile	Lab reference	Horizon	Charcoal (Taxon)	C-14 age (y BP)	$\delta^{13}C$ (‰)	Calibrated age 2σ (95.4%)
Moser et al. (2017)						
CL1	KIA45420	A2	Pinus group sylvestris	1051 ± 25	− 24.80 ± 0.14	1051–930
	KIA45421	A3	Deciduous Quercus	4200 ± 30	− 25.10 ± 0.15	4843–4627
	KIA47441(1)	A3	Pinus group sylvestris	2430 ± 30	− 21.91 ± 0.11	2699–2354
	KIA47441(2)	A3	n.i.	2695 ± 30	− 23.44 ± 0.19	2850–2755
	KIA50234(1)	A3	Pinus group sylvestris	3000 ± 40	− 23.86 ± 0.13	3316–3080
	KIA50234(2)	A3	n.i.	3020 ± 25	− 21.63 ± 0.14	3337–3083
	KIA48518	2Bw1	Deciduous Quercus	4065 ± 30	− 24.30 ± 0.17	4799–4437
	KIA48519(1)	2Bw1	Deciduous Quercus	4305 ± 25	− 24.52 ± 0.20	4960–4832
	KIA48519(2)	2Bw1	n.i.	4355 ± 30	− 24.36 ± 0.15	5032–4851
	KIA48520	2Bw1	Pinus group sylvestris	8895 ± 45	− 23.79 ± 0.17	10193–9794
CL2	POZ-59596	A1	Pinus group sylvestris	125 ± 30		273–10
	POZ-59597	A2	Pinus group sylvestris	155 ± 30		285–modern
	KIA48512	A2	Deciduous Quercus	2845 ± 25	− 27.77 ± 0.19	3056–2872
	KIA48513(1)	Bw	Abies	6760 ± 30	− 24.22 ± 0.13	7666–7576
	KIA48513(2)	Bw	n.i.	6675 ± 30	− 24.81 ± 0.13	7591–7489
	KIA48514	Bw	Juniperus	6975 ± 35	− 24.08 ± 0.22	7926–7705
	POZ-59598	Bw3	Juniperus	8270 ± 50		9430–9091
CL3	KIA48516	2Ab	Abies	8170 ± 50	− 24.93 ± 0.14	9269–9010
	KIA48515	2Ab	Deciduous Quercus	8920 ± 100	− 26.74 ± 0.11	10242–9695
	KIA48517	2Bwb	Deciduous Quercus	8820 ± 55	− 22.56 ± 0.12	10158–9682
CL4	KIA48507	A	Abies	3465 ± 35	− 23.97 ± 0.10	3834–3640
	KIA48508(1)	2Bw	Abies	8430 ± 40	− 24.88 ± 0.12	9530–9324
	KIA48508(2)	2Bw	n.i.	8525 ± 30	− 24.06 ± 0.16	9554–9453
	KIA48509	2Bw	Juniperus	12180 ± 60	− 21.52 ± 0.20	14245–13835
	KIA48510	2Bt	Abies	7245 ± 36	− 24.06 ± 0.26	8164–7982
CL5	POZ-59591	Ap	Fagus sylvatica	230 ± 30		421–modern
	POZ-59592	Bw1	Pinus group sylvestris	330 ± 30		473–308
	KIA48050	Bw2	Cornus	2015 ± 25	− 28.16 ± 0.21	2039–1895
	KIA48051(1)	Bw2	Juniperus	2865 ± 30	− 24.85 ± 0.14	3072–2879
	KIA48051(2)	Bw2	n.i.	2740 ± 30	− 24.24 ± 0.12	2920–2765
	KIA48051(3)	Bw2	n.i.	2465 ± 30	− 25.03 ± 0.25	2713–2379
	KIA48051(4)	Bw2	n.i.	2805 ± 30	− 23.38 ± 0.25	2995–2804
	POZ-59593	Bw2	Abies	2475 ± 30		2720–2380
	POZ-59595	C	Juniperus	5215 ± 35		6173–5908
	BETA - 320186	C	Juniperus	6480 ± 40	− 24.80 ± 0.00	7470–7310
	BETA - 320187	Ab	Leguminosae	810 ± 30	− 22.80 ± 0.00	781–681
	KIA48052(1)	Ab	Leguminosae	1250 ± 25	− 24.10 ± 0.20	1273–1084
	KIA48052(2)	Ab	n.i.	1240 ± 25	− 22.48 ± 0.13	1265–1075
	BETA - 320188	ABb	Abies	4130 ± 30		4821–4532
	KIA48053(1)	ABb	Deciduous Quercus	3510 ± 30	− 23.69 ± 0.15	3867–3697
	KIA48053(2)	ABb	n.i.	3455 ± 30	− 23.99 ± 0.15	3828–3640
	KIA48054	ABb	Juniperus	3810 ± 80	− 25.05 ± 0.23	4420–3981
Scarciglia et al. (2008)						
C1	DSA983		n.i.	342 ± 16		457–320
C2	DSA985		n.i.	3135 ± 18		3383–3355
C3	DSA986		n.i.	92 ± 24		254–modern
New measurements						
CL4	60–80 (1)	2Bw	n.i.	3565 ± 22	− 22.0 ± 1.0	3960–3734
	60–80 (2)	2Bw	n.i.	3620 ± 24	− 26.3 ± 1.0	4059–3852
CL5	80–90	Bw2	n.i.	6568 ± 26	− 28.8 ± 1.0	7555–7427

n.i. = not identified.

Table 8

Radiocarbon dating of the H_2O_2-resistant soil organic matter at the Nebrodi and Sila sites together with one additional site (CL5, Sila, according to Moser et al., 2017).

Soil	Horizon	Depth (cm)	Material	C-14 age (y BP)	$\delta^{13}C$ (‰)	Calibrated ages (cal BP)	
						1σ (68.2%)	2σ (95.4%)
Nebrodi I	A1	0–20	Volcanic soil	470 ± 30	− 14.0 ± 1.0	525–505	541–493
	A2	20–50	Volcanic soil	1565 ± 35	− 7.7 ± 1.0	1521–1411	1538–1381
Nebrodi III	A1	0–50	Volcanic soil	2850 ± 35	− 12.7 ± 1.0	3004–2884	3066–2867
	A2	50–75	Volcanic soil	4562 ± 29	− 15.9 ± 1.0	5315–5085	5437–5057
	Bw	75–110	Volcanic soil	8607 ± 35	− 21.2 ± 1.0	9595–9531	9662–9524
Nebrodi IV	A1	0–20	Volcanic soil	1810 ± 30	− 17.4 ± 1.0	1810–1709	1823–1628
Sila I	A1	0–20	Volcanic soil	725 ± 30	− 19.8 ± 1.0	686–663	725–570
	Bw	40–60	Volcanic soil	7345 ± 33	− 28.0 ± 1.0	8195–8051	8292–8030
Sila II	A1	0–20	Volcanic soil	380 ± 30	− 19.0 ± 1.0	500–333	505–319
CL5	Ab	130–150	Volcanic soil	1608 ± 23	− 22.1 ± 1.0	1545–1419	1553–1415

Table 9
Comparison of several chemical weathering indices along the investigated soil profiles: Index B (Kronberg and Nesbitt, 1981); molar (K + Ca)/Ti ratio (Egli et al., 2008); CIA = chemical index of alteration (Nesbitt and Young, 1982); CIW = chemical index of weathering (Harnois, 1988); PIA = plagioclase index of alteration (Fedo et al., 1995); WIP = weathering index of Parker (Parker, 1970; Price and Velbel, 2003); CPA = chemical proxy of alteration (Buggle et al., 2011).

Site	Horizon	Index B (−)	(K + Ca)/Ti (−)	CIA (%)	CIW (%)	PIA (%)	WIP (−)	CPA (%)
Nebrodi I	A1	0.33	3.30	67.2	73.2	70.5	42.0	84.3
	A2	0.30	2.91	69.9	76.3	73.9	41.9	85.6
	A3	0.30	2.93	70.4	76.7	74.4	40.8	86.1
	A4	0.31	2.99	69.5	75.4	73.1	43.8	85.0
	AB	0.29	5.06	70.7	79.2	76.3	47.8	87.0
	Bw	0.31	5.56	68.8	78.1	74.7	47.5	86.9
Nebrodi II	A1	0.33	4.14	67.4	73.9	71.1	40.0	87.4
	A2	0.28	3.11	71.6	77.0	75.2	36.6	88.6
	2BA	0.21	1.44	79.0	81.9	81.2	33.0	89.1
	2Bw	0.20	1.47	79.9	82.0	81.5	31.0	89.6
	3BC	0.27	3.25	72.8	81.7	79.1	23.6	87.5
	4BC	0.23	2.45	77.4	84.9	83.3	18.0	91.6
Nebrodi III	A1	0.33	5.53	67.5	77.0	73.3	48.6	83.4
	A2	0.25	2.59	75.0	81.8	80.0	42.0	87.4
	Bw	0.24	2.87	76.1	82.5	80.9	42.9	88.5
	2BCg	0.32	5.76	68.3	78.8	75.0	49.2	83.7
	2BC	0.31	6.44	69.4	80.4	76.7	47.7	85.9
	3BC	0.28	4.47	72.1	82.7	79.7	43.1	88.3
Nebrodi IV	A1	0.35	4.28	64.5	73.0	68.9	42.7	82.0
	A2	0.26	2.49	74.4	81.5	79.5	32.8	88.6
	2Btm	0.25	1.98	75.2	78.3	77.4	33.0	88.9
	3Co	0.33	3.03	67.5	69.4	68.5	44.5	84.7
	4Co	0.23	1.70	77.2	78.7	78.3	29.0	89.5
	5Co	0.32	3.66	68.1	77.3	73.7	34.3	84.5
	6C	0.24	2.67	76.1	85.7	83.6	17.5	92.3
Sila I	A1	0.32	5.65	67.6	74.3	71.5	45.3	86.4
	A2	0.32	6.04	67.8	74.8	71.9	46.2	87.3
	Bw	0.34	8.78	66.1	72.3	69.4	53.7	86.1
	2Bw	0.35	8.65	65.2	71.2	68.3	55.4	85.8
	2C	0.38	10.96	61.8	68.0	64.4	59.5	84.0
Sila II	A1	0.29	4.82	71.2	77.4	75.2	45.9	88.2
	A2	0.31	6.64	69.2	74.8	72.6	49.1	88.1
	Bw	0.36	9.78	63.9	68.9	66.3	57.4	84.5
	2Bw	0.37	10.37	63.0	67.5	65.0	64.1	82.1
	2C	0.36	10.21	63.8	68.7	66.1	58.5	84.8
Lapilli[a]	2BA	0.42	2.64	58.3	60.8	59.1	67.4	75.7
	2Bw	0.48	3.43	52.2	54.6	52.4	75.1	71.5
	2Bw	0.35	1.92	64.6	65.9	65.2	60.0	79.2
Bedrock[b]		0.81	66.91	18.7	19.4	16.4	104.4	85.6

[a] Lapilli of the Nebrodi II site.
[b] Bedrock average of the Monti Nebrodi sites.

$$y = 76.88e^{-9E-06x}$$
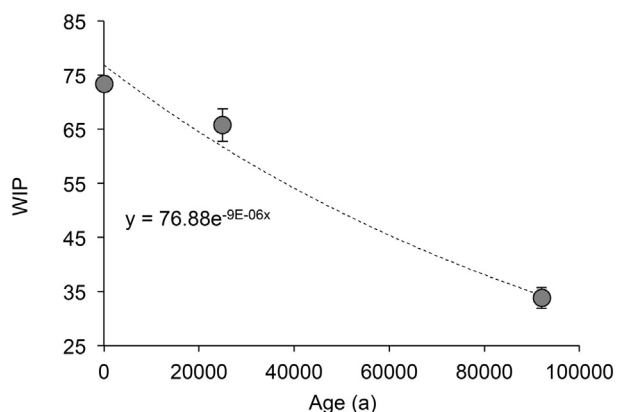
Fig. 9. Chronosequence based on data of Mirabella et al. (2005) that was used to estimate the ages of the volcanic deposits using the WIP (weathering index of Parker).

Table 10
Age estimation using the WIP (Parker, 1970; Price and Velbel, 2003). Data from Mirabella et al. (2005) was used for calibration (chemical data and numeric age indications are given) due to its close proximity to the investigation sites and favourable volcanic area. The calculation is based on the chemical composition of the A and AB (or Bw) horizons. The other horizons were excluded because they contain arenite, marl, lapilli (from the Etna) or granite (local bedrock). In addition, the timing of deposition was estimated using the chemical composition of volcanic clasts and glasses based on LA-ICP-MS measurements and SEM-EDS data (new and published data (Scarciglia et al., 2008; Vingiani et al., 2014)) and comparing them with the timing of eruptions and the evolution of the chemical composition (Si, Ti, REE) of eruptiva (Forni, 2011; Albert et al., 2013, 2017).

Site	Estimated soil ages (ka BP; based on WIP)	Estimated ages of volcanic deposits (ka BP; based on LA-ICP-MS)
Nebrodi I	62.3 ± 7.5	92–81; < 70
Nebrodi II	77.5 ± 6.9	
Nebrodi III	61.0 ± 8.8	
Nebrodi IV	80.0 ± 20.6	92–81; < 70
Average Nebrodi	70.2 ± 11.9	
Sila I	51.6 ± 10.4	
Sila II	46.6 ± 12.7	
Average Sila	49.1 ± 10.8	
Sila[a]		
Min	15.6	
Max	66.7	
average	45.3 ± 11.1	
Glass fragments Sila[a]		
Min	modern	< 70
Max	23.7	92–81

[a] Chemical data from Scarciglia et al. (2008), Vingiani et al. (2014).

Nb/Y vs Zr/Ti) or other trace elements (Co, Th) and rare earth elements (Ce, La). Besides the main geochemical composition (bulk soil), detailed geochemical data (major compounds, trace elements and REE) individual glass particles and volcanic clasts may contain important information about their origin (provided that geochemical data of the origin material exist). Immobile and trace elements systematics revealed that a large part of the volcanic sediments deposited at the investigated sites (Nebrodi and Sila mountains) most likely originate from the Aeolian Islands (Lipari, Vulcano). Larger particles (lapilli) in the Nebrodi soils have their origin from eruptions of the Etna. To better identify the source of origin isotopic ratios (e.g. $^{143}Nd/^{144}Nd$ vs $^{87}Sr/^{86}Sr$ or $^{208}Pb/^{204}/Pb$ vs $^{206}Pb/^{204}Pb$) should be investigated to better cope with weathering processes. LA-ICP-MS and SEM-EDS measurements gave a clear hint that several sources exist: not only the Aeolian Islands but also specific eruption epochs of the Etna (Biancavilla) contributed to the deposits.

The age estimate of these deposits has some limitations. Since radiocarbon dating appears to only give minimum ages (Early Holocene or Late Pleistocene) in this setting, we suggested that weathering indices and the chemical composition of volcanic glasses and clasts can be helpful for establishing a semi-quantitative dating and chronology. Our weathering index approach, combined with the geochemical fingerprinting, implies that large parts of the soils derive from the epochs VI to IX of Lipari, with possible influence from Vulcano (or Stromboli). This again shows that the volcanic soils consist of multiple deposits giving rise to a complex landscape evolution for the last 50 ka in the Sila mountains and 70 ka in the Nebrodi mountains. Although the age estimates seem reasonable, the results should be evaluated in the future by other, if possible numerical dating techniques.

The geochemical fingerprinting method used here could identify the sources of the deposits relatively precisely. While the weathering index-derived ages remain speculative, they do represent an improvement on previous chronologies in the area.
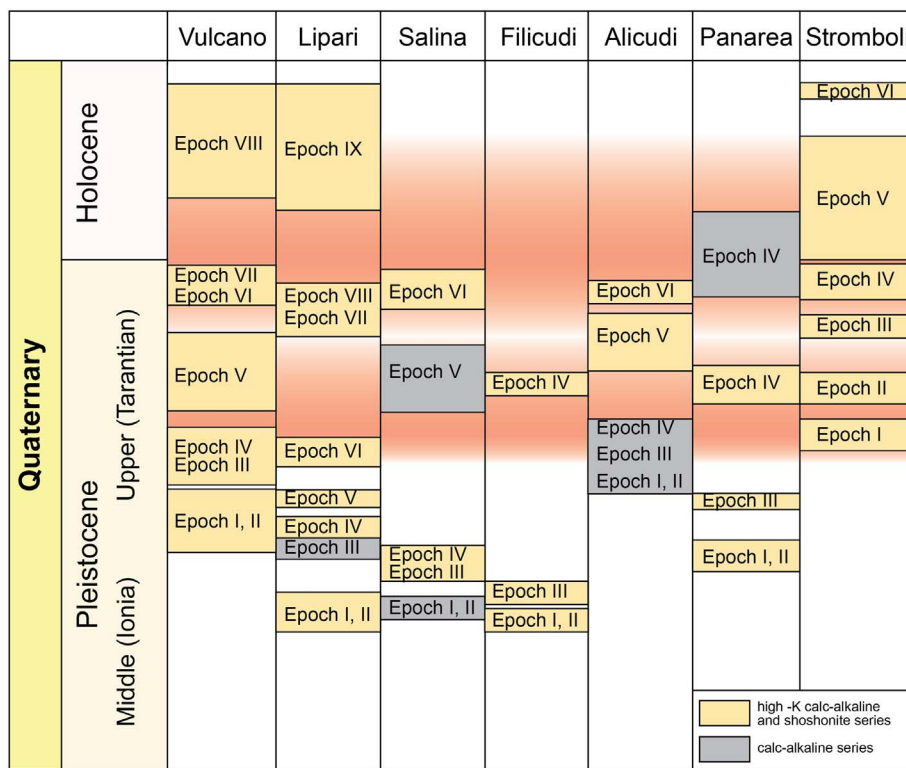
Fig. 10. Active periods of Aeolian Arc volcanism (in grey and yellow) according to Pichler (1989) and updated after Forni et al. (2013), De Astis et al. (2013), Lucchi et al. (2013a, 2013b, 2014a, 2014b) and Francalanci et al. (2013). The estimated age ranges of the volcanic deposits at the investigation sites (Sila and Nebrodi) using the WIP (weathering index after Parker) and chemical composition of glass particles, pumice and volcanic clasts are indicated in red stripes. (For interpretation of the references to colour in this figure legend, the reader is referred to the web version of this article.)

Table 11

Mass balance calculations (fine earth) and estimation of the volcanic proportion in the soil layers using several potential sources: 1)–3) Aeolian islands, Lipari (different eruption epochs) and 4) Biancavilla ignimbrite and Plinian eruptions, Etna.

Site	Horizon	Soil depth cm	Al_2O_3 kg/m²	TiO_2 kg/m²	[1]Volcanic proportion Lipari (epoch 6)	[2]Volcanic proportion (Lipari, < 50 ka; Albert et al., 2017)	[3]Volcanic proportion (Lipari; > ca. 30 ka; Mirabella et al., 2005)	[4]Volcanic proportion Biancavilla(Albert et al., 2013)
Nebrodi I	A1	0–20	35.03	2.08	100%	0%	100%	80%
	A2	20–50	58.91	3.42	100%	0%	100%	76%
	A3	50–90	79.45	4.58	100%	0%	100%	75%
	A4	90–130	88.66	5.08	100%	0%	100%	74%
	AB	130–140	29.85	1.01	28%	0%	15%	6%
	Bw	140–160	57.66	2.03	46%	0%	25%	11%
Nebrodi II	A1	0–15	28.42	1.52	47%	25%	63%	0%
	A2	15–50	68.64	3.84	31%	16%	42%	0%
	2BA	50–65	31.87	2.07	0%	0%	0%	0%
	2Bw	65–90	30.85	1.84	0%	0%	0%	0%
Nebrodi III	A1	0–50	112.83	3.72	18%	0%	10%	4%
	A2	50–75	55.71	2.65	100%	100%	100%	46%
	Bw	75–110	91.08	3.81	100%	72%	70%	30%
Nebrodi IV	A1	0–20	23.96	1.2	65%	37%	84%	0%
	A2	20–35	20.29	1.13	41%	23%	53%	0%
	2Btm	35–115	170.78	11.51	0%	0%	0%	0%
	2C	115–135	35.86	2.34	0%	0%	0%	0%
Sila I	A1	0–20	39.22	1.45	85%	0%	63%	35%
	A2	20–40	43.9	1.56	76%	0%	56%	31%
	Bw	40–60	54.62	1.42	5%	0%	4%	2%
	2Bw	60–80	65.53	1.82	21%	0%	14%	7%
	2C	80–100	57.09	1.45	0%	0%	0%	0%
Sila II	A1	0–20	40.9	1.49	85%	0%	65%	38%
	A2	20–40	39.38	1.2	49%	0%	35%	19%
	Bw	40–60	48.65	1.23	6%	0%	4%	2%
	2Bw	60–80	60.52	1.4	0%	0%	0%	0%
	2C	80–100	49.39	1.22	0%	0%	0%	0%

[1] Average composition (data from Forni, 2011)
Al_2O_3: 169 ± 4.9 g/kg
TiO_2: 6.7 ± 0.5 g/kg.
[2] Average composition (data from Albert et al., 2017)
Al_2O_3: 131 ± 6.8 g/kg
TiO_2: 1.0 ± 0.4 g/kg.
[3] Average composition (data from Mirabella et al., 2005)
Al_2O_3: 170 ± 27.2 g/kg
TiO_2: 7.9 ± 6.2 g/kg.
[4] Using the Biancavilla ignimbrite and unit D Plinian fall deposits (Etna) as origin (Albert et al., 2013)
Al_2O_3: 172 ± 3.7 g/kg
TiO_2: 11.4 ± 1.9 g/kg.

Acknowledgements

References

Albert, P.G., Tomlinson, E.L., Lane, C.S., Wulf, S., Smith, V.C., Coltelli, M., Keller, J., Lo Castro, D., Manning, C.J., Müller, W., Menzies, M.A., 2013. Late glacial explosive activity on Mount Etna: implications for proximal–distal tephra correlations and the synchronisation of Mediterranean archives. J. Volcanol. Geotherm. Res. 265, 9–26.

Albert, P.G., Tomlinson, E.L., Smith, V.C., Di Traglia, F., Pistolesi, M., Morris, A., Donato, P., De Rosa, R., Sulpizio, R., Keller, J., Rosi, M., Menzies, M., 2017. Glass geochemistry of pyroclastic deposits from the Aelian Islands in the last 50 ka: a proximal database for tephrochronology. J. Volcanol. Geotherm. Res. 336, 81–107.

Beckhoff, B., Kanngießer, B., Langhoff, N., Wedell, R., Wolff, H., 2006. Handbook of Practical X-ray Fluorescence Analysis. Springer, Berlin.

Bertagnini, A., Méltrich, N., Francalanci, L., Landi, P., Tommasini, S., Conticelli, S., 2008. Volcanology and magma geochemistry of the present-day activity: constraints on the feeding system. In: Calvari, S., Inguaggiato, S., Puglisi, G., Ripepe, M., Rosi, M. (Eds.), The Stromboli Volcano: An Integrated Study of the 2002–2003 Eruption. American Geophysical Union, Washington, D. C., pp. 19–37.

Bourne, A.J., Albert, P.G., Matthews, I.P., Trincardi, F., Wulf, S., Asioli, A., Blockley, S.P.E., Keller, J., Lowe, J.J., 2015. Tephrochronology of core PRAD 1-2 from the Adriatic Sea: insights into Italian explosive volcanism for the period 200–80 ka. Quat. Sci. Rev. 116, 28–43.

Brock, F., Higham, T., Ditchfield, P., Bronk Ramsey, C., 2010. Current pretreatment methods for AMS radiocarbon dating at the Oxford radiocarbon accelerator unit (ORAU). Radiocarbon 52, 103–112.

Bronk Ramsey, C., 2001. Development of the radiocarbon calibration program. Radiocarbon 43, 355–363.

Bronk Ramsey, C., 2009. Bayesian analysis of radiocarbon dates. Radiocarbon 51, 337–360.

Buggle, B., Glaser, B., Hambach, U., Gerasimenko, N., Markovic, S., 2011. An evaluation of geochemical weathering indices in loess-paleosol studies. Quat. Int. 240, 12–21.

Carcaillet, C., Brun, J.-J., 2000. Changes in landscape structure in the northwestern Alps over the last 7000 years: lessons from soil charcoal. J. Veg. Sci. 11, 705–714.

Cirrincione, R., Fazio, E., Fiannacca, P., Ortolano, G., Pezzino, A., Punturo, R., 2015. The Calabria-Peloritani Orogen, a composite terrane in Central Mediterranean; its overall architecture and geodynamic significance for a pre-Alpine scenario around the Tethyan basin. Periodico Mineral. 84-3B (Special Issue), 701–749.

Condomines, M., Tanguy, J.C., 1995. Magma dynamics at Mt Etna: constraints from U–Th–Ra–Pb radioactive disequilibria and Sr isotopes in historical lavas. Earth Planet. Sci. Lett. 132, 25–41.

Costantini, E., Dazzi, C. (Eds.), 2013. The Soils of Italy. Springer, Dordrecht, Heidelberg, New York, London.

Dahms, D., Favilli, F., Krebs, R., Egli, M., 2012. Soil weathering and accumulation rates of oxalate-extractable phases derived from alpine chronosequences of up to 1 Ma in age. Geomorphology 151, 99–113.

De Astis, G., Lucchi, F., Dellino, P., La Volpe, L., Tranne, C.A., Frezzoti, M.L., Peccerillo, A., 2013. Chapter 11 Geology, volcanic history and petrology of Vulcano (central Aeolian archipelago). In: Lucchi, F., Peccerillo, A., Keller, J., Tranne, C.A., Rossi, P.L. (Eds.), The Aeolian Islands Volcanoes. The Geological Society of Londonpp. 281–349.

De Rosa, R., Donato, P., Scarciglia, F., 2016. On the origin and post-depositional history of widespread massive ash deposits: the case of Intermediate Brown Tuffs (IBT) of Lipari (Aeolian Islands, Italy). J. Volcanol. Geotherm. Res. 327, 135–151.

Egli, M., Fitze, P., 2000. Formulation of pedologic mass balance based on immobile elements: a revision. Soil Sci. 165, 437–443.

Egli, M., Nater, M., Mirabella, A., Raimondi, S., Plötze, M., Alioth, L., 2008. Clay minerals, oxyhydroxide formation, element leaching and humus development in volcanic soils. Geoderma 143, 101–114.

Egli, M., Gristina, L., Wiesenberg, G., Martin Civantos, J.M., Rotolo, A., Novara, A., Brandová, D., Raimondi, S., 2013. From pedologic indications to archaeological reconstruction: deciphering land use in the Islamic period in the Baida district (northwestern Sicily). J. Archaeol. Sci. 40, 2670–2685.

Eusterhues, K., Rumpel, C., Kögel-Knabner, I., 2005. Stabilization of soil organic matter isolated via oxidative degradation. Org. Geochem. 36, 1567–1575.

Favilli, F., Egli, M., Cherubini, P., Sartori, F., Haeberli, W., Delbos, E., 2008. Comparison of different methods of obtaining a resilient organic matter fraction in Alpine soils. Geoderma 245, 355–369.

Favilli, F., Egli, M., Brandova, D., Ivy-Ochs, S., Kubik, P., Cherubini, P., Mirabella, A., Sartori, G., Giaccai, D., Haeberli, W., 2009a. Combined use of relative and absolute dating techniques for decting signals of Alpine landscape evolution during the late Pleistocene and early Holocene. Geomorphology 112, 48–66.

Favilli, F., Egli, M., Brandová, D., Ivy-Ochs, S., Kubik, P.W., Maisch, M., Cherubini, P., Haeberli, W., 2009b. Combination of numerical dating techniques using [10]Be in rock boulder and ^{14}C of resilient soil organic matter for reconstructing the chronology of glacial and periglacial processes in a high alpine catchment during the late Pleistocene and early Holocene. Radiocarbon 51, 537–552.

Favilli, F., Cherubini, P., Collenberg, M., Egli, M., Sartori, G., Schoch, W., Haeberli, W., 2010. Charcoal fragments of Alpine soils as an indicator of landscape evolution during the Holocene in Val di Sole (Trentino, Italy). The Holocene 20, 67–79.

Fedo, C.M., Nesbitt, H.W., Young, G.M., 1995. Unraveling the effects of potassium metasomatism in sedimentary rocks and paleosols, with implications for paleoweathering conditions and provenance. Geology 23, 921–924.

Fisher, R.V., Schmincke, H.U., 1984. Pyroclastic Rocks. Springer, Berlin.

Forni, F., 2011. Petrology and Geochemistry of Lipari Island (Aeolian Archipelago): Constraints on Magma Genesis and Evolution. PhD thesis University of Bologna, Italy.

Forni, F., Lucchi, F., Peccerillo, A., Tranne, C.A., Rossi, P.L., Frezzotti, M.L., 2013. Chapter 10 Stratigraphy and geological evolution of the Lipari volcanic complex (central Aeolian archipelago). In: Lucchi, F., Peccerillo, A., Keller, J., Tranne, C.A., Rossi, P.L. (Eds.), The Aeolian Islands Volcanoes. The Geological Society of Londonpp. 213–279.

Francalanci, L., Lucchi, F., Keller, J., De Astis, G., Tranne, C.A., 2013. Chapter 13 Eruptive volcano-tectonic and magmatic history of the Stromboli volcano (north-eastern Aeolian archipelago). In: Lucchi, F., Peccerillo, A., Keller, J., Tranne, C.A., Rossi, P.L. (Eds.), The Aeolian Islands Volcanoes. The Geological Society of Londonpp. 397–471.

Giaccio, B., Isaia, R., Sulpizio, R., Zanchetta, G., 2008. Explosive volcanism in the central Mediterranean area during the late Quaternary-linking sources and distal archives. J. Volcanol. Geotherm. Res. 177, v–vii.

Glenn, R.C., Nash, V.E., 1964. Weathering relationship between gibbsite, kaolinite, chlorite, and expansible layer silicates in selected soils from the lower Mississippi Coastal Plain. Clays Clay Miner. Proc. 12, 539–548.

Guillong, M., Meier, D.L., Allan, M.M., Heinrich, C.A., Yardley, B.W.D., 2008. SILLS: a MATLAB-based program for the reduction of laser ablation ICP-MS data of homogeneous materials and inclusions. In: Sylvester, P. (Ed.), Laser Ablation ICP-MS in the Earth Sciences: Current Practices and Outstanding Issues. Mineral. Mineralogical Association of Canada Short Course Series Vol. 40. pp. 328–333.

Harnois, L., 1988. The CIW index: a new chemical index of weathering. Sediment. Geol. 55, 319–322.

Hastie, A.R., Kerr, A.C., Pearce, J.A., Mitchell, S.F., 2007. Classification of altered volcanic island arc rocks using immobile trace elements: development of the Th–Co discrimination diagram. J. Petrol. 48, 2341–2357.

IUSS Working Group WRB, 2015. World Reference Base for Soil Resources 2014, Update 2015. International Soil Classification System for Naming Soils and Creating Legends for Soil Maps. World Soil Resources Reports 106 FAO, Rome.

Johannsen, A., 1937. A descriptive petrography of the igneous rocks. In: Introduction, Textures, Classifications, and Glossary. Vol. 1 The University of Chicago Press, Chicago, Illinois.

Joplin, G.A., 1968. The shoshonite association: a review. J. Geol. Soc. Aust. 15, 275–294.

Karkanas, P., Bar-Yosef, O., Goldberg, P., Weiner, S., 2000. Diagenesis in prehistoric caves: the use of minerals that form in situ to assess the completeness of the archaeological record. J. Archaeol. Sci. 27, 915–929.

Keller, J., Ryan, W.B.F., Ninkovich, D., Altherr, R., 1978. Explosive volcanic activity in the Mediterranean over the past 200,000 yr as recorded in deep-sea sediments. Geol. Soc. Am. Bull. 89, 591–604.

Kleber, M., Sollins, P., Sutton, R., 2007. A conceptual model of organo-mineral interactions in soils: self-assembly of organic molecular fragments into zonal structures on mineral surfaces. Biogeochemistry 85, 9–24.

Kronberg, G.I., Nesbitt, H.W., 1981. Quantification of weathering of soil chemistry and soil fertility. J. Soil Sci. 32, 453–459.

de Lafontaine, G., Couillard, P., Payette, S., 2011. Permineralization process promotes preservation of Holocene macrofossil charcoal in soils. J. Quat. Sci. 26, 571–575.

Le Pera, E., Sorriso-Valvo, M., 2000. Weathering and morphogenesis in a Mediterranean climate Clabria, Italy. Geomorphology 34, 251–270.

Lucchi, F., Tranne, C.A., Peccerillo, A., Keller, J., Rossi, P.L., 2013a. Chapter 12 Geological history of the Panarea volcanic group (eastern Aeolian archipelago). In: Lucchi, F., Peccerillo, A., Keller, J., Tranne, C.A., Rossi, P.L. (Eds.), The Aeolian Islands Volcanoes. The Geological Society of Londonpp. 351–395.

Lucchi, F., Gertisser, R., Keller, J., Forni, F., De Astis, G., Tranne, C.A., 2013b. Chapter 9 Eruptive history and magmatic evolution of the island of Salina (central Aeolian archipelago). In: Lucchi, F., Peccerillo, A., Keller, J., Tranne, C.A., Rossi, P.L. (Eds.), The Aeolian Islands Volcanoes. The Geological Society of Londonpp. 155–211.

Lucchi, F., Santo, A.P., Tranne, C.A., Peccerillo, A., Keller, J., 2014a. Chapter 8 Volcanism, magmatism, volcano-tectonic and sea-level fluctuations in the geological history of Filicudi (western Aeolian archipelago). In: Lucchi, F., Peccerillo, A., Keller, J., Tranne, C.A., Rossi, P.L. (Eds.), The Aeolian Islands Volcanoes. The Geological Society of Londonpp. 113–153.

Lucchi, F., Peccerillo, A., Tranne, C.A., Rossi, P.L., Frezzotti, M.L., Donati, D., 2014b. Chapter 7 Volcanism, calderas and magmas of the Alicudi composite volcano (western Aeolian archipelago). In: Lucchi, F., Peccerillo, A., Keller, J., Tranne, C.A., Rossi, P.L. (Eds.), The Aeolian Islands Volcanoes. The Geological Society of Londonpp. 83–111.

Lynch, J.A., Clark, J.S., Stocks, B.J., 2004. Charcoal production, dispersal, and deposition from Fort Providence experimental fire: interpreting fire regimes from charcoal record in boreal forests. Can. J. For. Res. 34, 1642–1656.

McKeague, J.A., Brydon, J.E., Miles, N.M., 1971. Differentiation of forms of extractable iron and aluminium in soils. Soil Sci. Soc. Am. Proc. 35, 33–38.

Mirabella, A., Egli, M., Raimondi, S., Giaccai, D., 2005. Origin of clay minerals in soils on pyroclastic deposits in the island of Lipari (Italy). Clay Clay Miner. 53, 410–422.

Mizota, C., van Reeuwijk, L.P., 1989. Clay mineralogy and chemistry of soils formed in volcanic material in diverse climate regions. In: International Soil Reference and Information Centre. Soil Monograph Vol. 2 (Wageningen).

Morrison, G.W., 1980. Characteristics and tectonic setting of the shoshonite rock association. Lithos 13, 97–108.

Moser, D., Di Pasquale, G., Scarciglia, F., Nelle, O., 2017. Holocene mountain forest changes in central Mediterranean: soil charcoal data from the Sila Massif (Calabria, southern Italy). Quat. Int.. http://dx.doi.org/10.1016/j.quaint.2017.01.042. (under

review).

Munno, R., Rossi, G., Tadini, C., 1980. Crystal chemistry of kimzeyite from Stromboli, Aeolian Islands, Italy. Am. Mineral. 65, 188–191.

Narcisi, B., Vezzoli, L., 1999. Quaternary stratigraphy of distal tephra layers in the Mediterranean an overview. Glob. Planet. Chang. 21, 31–50.

Nesbitt, H.W., Young, G.M., 1982. Early Proterozoic climates and plate motions inferred from major element chemistry of lutites. Nature 299, 715–717.

Parker, A., 1970. An index for weathering for silicate rocks. Geol. Mag. 107, 29–147.

Paterne, M., Guichard, F., Labeyrie, J., 1988. Explosive activity of the south Italian volcanoes during the past 80,000 years as determined by marine tephrochronology. J. Volcanol. Geotherm. Res. 34, 153–172.

Paterne, M., Guichard, F., Duplessy, J.C., Siani, G., Sulpizio, R., Labeyrie, J., 2008. A 90,000–200,000 yrs marine tephra record of Italian volcanic activity in the Central Mediterranean Sea. J. Volcanol. Geotherm. Res. 177, 187–196.

Pearce, J.A., 1996. A user's guide to basalt discrimination diagrams. In: Wyman, D.A. (Ed.), Trace Element Geochemistry of Volcanic Rocks: Applications for Massive Sulphide Exploration. Geological Association of Canada, Short Course Notes Vol. 12. pp. 79–113.

Peccerillo, A., 2005. Plio-Quaternary Volcanism in Italy. Springer, Berlin.

Pelle, T., Scarciglia, F., Di Pasquale, G., Allevato, E., Marino, D., Robustelli, G., La Russa, M.F., Pulice, I., 2013. Multidisciplinary study of Holocene archaeological soils in an upland Mediterranean site: natural versus anthropogenic environmental changes at Cecita Lake, Calabria, Italy. Quat. Int. 303, 163–179.

Peters, D., Pettke, T., 2017. Evaluation of major to ultra-trace element bulk rock chemical analysis of nanoparticulate pressed powder pellets by LA-ICP-MS. Geostand. Geoanal. Res. 41, 5–28.

Pettke, T., Oberli, F., Audetat, A., Guillong, M., Simon, A., Hanley, J., Klemm, L.M., 2012. Recent developments in element concentration and isotope ratio analysis of individual fluid inclusions by laser ablation single and multiple collector ICP–MS. Ore Geol. Rev. 44, 10–38.

Pichler, H., 1967. Neue Erkenntnisse über Art und Genese des Vulkanismus der Äolischen Inseln (Sizilien). Geologische Rundschau Stuttgart 57, 102–126.

Pichler, H., 1981. Sammlung Geologischer Führer 69, Lipari, Vulcano, Stromboli, Tyrrhenisches Meer Italienische Vulkan-Gebiete III. Gebrüder Borntträger, Berlin-Stuttgart.

Pichler, H., 1984. Sammlung Geologischer Führer Ätna, Sizilien. Italienische Vulkan-Gebiete IV. Gebrüder Borntträger, Berlin-Stuttgart.

Pichler, H., 1989. Sammlung Geologischer Führer: Italienische Vulkangebiete V. Mte. Vulture, Äolische Inseln II (Saline, Filicudi, Alicudi, Panarea), Mti. Iblei, Capo Passero, Ustica, Pantelleria und Linosa. Gebrüder Borntträger, Berlin-Stuttgart.

Plante, A.F., Chenu, C., Balabane, M., Mariotti, A., Righi, D., 2004. Peroxide oxidation of clay associated organic matter in a cultivation chronosequence. Eur. J. Soil Sci. 55, 471–478.

Price, J.R., Velbel, M.A., 2003. Chemical weathering indices applied to weathering profiles developed on heterogeneous felsic metamorphic parent rocks. Chem. Geol. 202, 397–416.

Reimer, P.J., Bard, E., Bayliss, A., Beck, J.W., Blackwell, P.G., Bronk Ramsey, C., Buck, C.E., Cheng, H., Edwards, R.L., Friedrich, M., Grootes, P.M., Guilderson, T.P., Haflidason, H., Hajdas, I., Hatté, C., Heaton, T.J., Hoffmann, D.L., Hogg, A.G.,

Hughen, K.A., Kaiser, K.F., Kromer, B., Manning, S.W., Nui, M., Reimer, R.W., Richards, D.A., Scott, E.M., Southon, J.R., Staff, R.A., Turney, C., van der Plicht, J., 2013. IntCal13 and Marine13 radiocarbon age calibration curves 0–50,000 years cal BP. Radiocarbon 55, 1869–1887.

Sandri, L., Costa, A., Selva, J., Tonini, R., Macedonio, G., Folch, A., Sulpizio, R., 2016. Beyond eruptive scenarios: assessing tephra fallout hazard from Neapolitan volcanoes. Sci Rep 6 (24271), 1–13.

Scarciglia, F., De Rosa, R., Vecchio, G., Apollaro, C., Robustelli, G., Terrasi, F., 2008. Volcanic soil formation in Calabria (southern Italy): the Cecita Lake geosol in the late Quaternary geomorphological evolution of the Sila uplands. J. Volcanol. Geotherm. Res. 177, 101–117.

Siddig, A.A., Ellison, A.M., Ochs, A., Villar-Leeman, C., Lau, M.K., 2015. How do ecologists select and use indicator species to monitor ecological change? Insights from 14 years of publication in ecological indicators. Ecol. Indic. 60, 223–230.

Soil Survey Division Staff, 2010. Keys to Soil Taxonomy. US Department of Agriculture (USDA) and National Resource Conservation Service (NRCS), Washington.

Sommer, M., Halm, D., Weller, U., Zarei, M., Stahr, K., 2000. Lateral podzolization in a granite landscape. Soil Sci. Soc. Am. J. 64, 1434–1442.

Stiles, C.A., Mora, C.I., Driesse, S.G., 2003. Pedogenetic processes and domain boundaries in a ertisol climosequence: evidence from titanium and zirconium distribution and morphology. Geoderma 116, 279–299.

Sulpizio, R., Zanchetta, G., Caron, B., Dellino, P., Mele, D., Giaccio, B., Insinga, D., Paterne, M., Siani, G., Costa, A., Macedonio, G., Santacroce, R., 2014. Volcanic ash hazard in the Central Mediterranean assessed from geological data. Bull. Volcanol. 76, 866.

Sumner, M.E. (Ed.), 1999. Handbook of Soil Science. CRC press, Boca Raton.

Sun, S.S., McDonough, W.F., 1989. Chemical and isotopic systematics of oceanic basalts; implications for mantle composition and processes. In: Saunders, A.D., Norry, M.J. (Eds.), Magmatism in the Ocean Basins. Geological Society Special Publication Vol. 42. Blackwell Scientific, Oxford, pp. 313–345.

Thomas, M.F.H., 2011. Sedimentology and Basin Context of the Numidian Flysch Formation; Sicily and Tunisia. Doctoral Thesis 85.

Torn, M.S., Trumbore, S.E., Chadwick, O.A., Vitousek, P.M., Hendricks, D.M., 1997. Mineral control of soil organic carbon storage and turnover. Nature 389, 170–173.

Tuttolomondo, T., Licata, M., Leto, C., Bonsangue, G., Gargano, M.L., Venturella, G., La Bella, S., 2014. Popular uses of wild plant species for medicinal purposes in the Nebrodi Regional Park (north-eastern Sicily, Italy). J. Ethnopharmacol. 157, 21–37.

Vingiani, S., Scarciglia, F., Mileti, F.A., Donato, P., Terribile, F., 2014. Occurrence and origin of soils with andic properties in Calabria (southern Italy). Geoderma 232, 500–516.

Weiner, S., Goldberg, P., Bar-Yosef, O., 1993. Bone preservation in Kebara Cave, Israel, using on-site Fourier transform infrared spectrometry. J. Archaeol. Sci. 20, 613–627.

Wood, R.E., Douka, K., Boscato, P., Haeserts, P., Sinitsyn, A., Higham, T.F.G., 2012. Testing the ABOx-SC method: dating known-age charcoals associated with the Campanian ignimbrite. Quat. Geochronol. 9, 16–26.

Zimmerer, M.J., Lafferty, J., Coble, M.A., 2016. The eruptive and magmatic history of the youngest pulse of volcanism at the Valles caldera: implications for successfully dating late quaternary eruptions. J. Volcanol. Geotherm. Res. 310, 50–57.